

Termination of typical wavefunction multifractal spectra at the Anderson metal-insulator transition: Field theory description using the functional renormalization group

Matthew S. Foster,^{1,2,*} Shinsei Ryu,³ and Andreas W. W. Ludwig⁴

¹*Physics Department, Columbia University, New York, NY 10027, USA*

²*Department of Physics and Astronomy, Rutgers University, Piscataway, NJ 08854, USA*

³*Department of Physics, University of California, Berkeley, CA 94720, USA*

⁴*Department of Physics, University of California, Santa Barbara, CA 93106, USA*

(Dated: November 4, 2018)

We revisit the problem of wavefunction statistics at the Anderson metal-insulator transition (MIT) of non-interacting electrons in $d > 2$ spatial dimensions. At the transition, the complex spatial structure of the critical wavefunctions is reflected in the non-linear behavior of the multifractal spectrum of generalized inverse participation ratios (IPRs). Beyond the crossover from narrow to broad IPR statistics, which always occurs for sufficiently large moments of the wavefunction amplitude, the spectrum obtained from a *typical* wavefunction associated with a particular disorder realization differs markedly from that obtained from the *disorder-averaged* IPRs. This phenomenon is known as the termination of the multifractal spectrum. We provide a field theoretical derivation for the termination of the typical multifractal spectrum, by combining the non-linear sigma model framework, conventionally used to access the MIT in $d = 2 + \epsilon$ dimensions, with a functional renormalization group (FRG) technique. The FRG method deployed here was originally pioneered to study the properties of the two-dimensional (2D) random phase XY model [D. Carpentier and P. Le Doussal, Nucl. Phys. B **588**, 565 (2000)]. The same method was used to demonstrate the termination of the multifractal spectrum in the very special problem of 2D Dirac fermions subject to a random Abelian vector potential. Our result shows that the *typical* multifractal wavefunction spectrum and its termination can be obtained at a generic Anderson localization transition in $d > 2$, within the standard field theoretical framework of the non-linear sigma model, when combined with the FRG.

I. INTRODUCTION

Quantum interference induced by multiple elastic impurity scattering can produce very complex spatial fluctuations in electronic wavefunctions. The statistics of these fluctuations may be used to distinguish different regimes of qualitative wavefunction behavior, e.g. localized versus extended. Of particular interest are the wavefunction statistics at a delocalization transition, such as the Anderson metal-insulator transition (MIT)¹ at the mobility edge in three spatial dimensions,^{2,3} or the integer quantum Hall plateau (IQHP) transition in two dimensions.^{3,4,5} Here, the spatial structure of the critical wavefunctions is known not to be characterized by just a single (or a few) independent exponent(s), but by an infinite set thereof ('multifractality'). More precisely, wavefunction statistics are encoded through the $\tau(q)$ spectrum, or its Legendre transform, the singularity spectrum $f(\alpha)$.^{2,3,4,5,6,7}

The $\tau(q)$ spectrum is defined via the (generalized) inverse participation ratio (IPR),⁸ given by

$$P_q(\varepsilon_i) \equiv \int_{L^d} d^d \mathbf{r} |\psi_i(\mathbf{r})|^{2q}, \quad P_q \sim L^{-\tau(q)}, \quad (1.1)$$

where d is the spatial dimensionality of the system, L^d denotes the system volume, and $|\psi_i(\mathbf{r})|^2$ is the probability density of a normalized eigenstate wavefunction $\psi_i(\mathbf{r})$ with energy ε_i , evaluated at the point \mathbf{r} . For eigenenergies ε lying within a band of extended plane wave states,

$\tau(q) = d(q-1)$, while exponentially localized states yield $\tau(q) \sim 0$ for $L \gg \xi$, with ξ the localization length. Multifractal behavior refers to non-linear q -dependence of the $\tau(q)$ spectrum, and occurs, e.g., at the mobility edge $\varepsilon = \varepsilon_c$ in a disordered three-dimensional (3D) system of non-interacting electrons.⁹ The singularity spectrum $f(\alpha)$ is related to the $\tau(q)$ spectrum through the Legendre transformation,

$$f(\alpha) = q\alpha - \tau(q), \quad \frac{d\tau(q)}{dq} = \alpha. \quad (1.2)$$

The set of points at which an eigenfunction takes the value $|\psi(\mathbf{r})|^2 \sim L^{-\alpha}$ is distributed according to the weight $L^{f(\alpha)}$;^{4,10} in this sense, the singularity spectrum characterizes the interwoven fractal measures of the sample associated with differently-scaling components of wavefunction intensity. The wavefunction statistics have been studied experimentally using thin microwave cavities;¹¹ a very broad distribution of the wavefunction intensity, indicative of multifractal behavior, was indeed observed.^{2,6,12}

The multifractal spectrum $[\tau(q)$ or $f(\alpha)]$ at a delocalization critical point is universal, and thus serves as a "fingerprint" of the spatial structure of wavefunctions. Spectra have been computed numerically at myriad delocalization transitions occurring in various spatial dimensions; see e.g. Refs. 4,5,13,14,15,16,17,18,19,20,21. In particular, extensive numerical studies of the IQHP transition^{5,14,16} employing different microscopic models

have convincingly established the universality of the entire $f(\alpha)$ spectrum. Recent work includes that of Refs. 18 and 19, which aim in part at decrypting the critical (conformal field) theory describing the plateau transition.

To compute the entire multifractal spectrum analytically is, however, a very difficult task in generic systems. This is even more so because it is a non-analytic function of q or α . As emphasized in Refs. 22, 23, and 3, this non-analyticity is related to the fact that the $\tau(q)$ and $f(\alpha)$ spectra are defined for a *typical* representative wavefunction, drawn in principle from a system in a single, fixed realization of the static disorder. On the contrary, analytical methods (i.e., those based upon field theories) are best suited for calculating quenched *averaged* quantities. To be precise, we define, following Ref. 23, *two* sets of multifractal statistics in terms of the IPR defined in Eq. (1.1):

$$\tau(q) \equiv -\frac{d\overline{\ln P_q}}{d\ln L}, \quad (1.3a)$$

$$\tilde{\tau}(q) \equiv -\frac{d\ln \overline{P_q}}{d\ln L}. \quad (1.3b)$$

In this equation, the overbar $\overline{\dots}$ represents an average over realizations of the quenched disorder. The typical $\tau(q)$ spectrum in Eq. (1.1) obtains from the log of the IPR for a representative wavefunction; since the latter quantity is expected to be self-averaging at the delocalization transition,^{15,23} we may introduce an additional, though redundant ensemble average over disorder realizations, as in Eq. (1.3a). We have also defined $\tilde{\tau}(q)$ in Eq. (1.3b), which obtains from the average of the IPR itself. The averaged IPR can be encoded through the moments of the local density of states (LDOS) operator in an effective low-energy field theory (see Sec. II, below); then, the scaling dimensions of the LDOS moment operators directly determine $\tilde{\tau}(q)$. No such effectively local construction exists for the typical spectrum $\tau(q)$, and in fact “non-local” (or more precisely, “multilocal”) correlations play an essential role^{24,25,26,27} in the “termination” (defined below) of the typical $\tau(q)$, as we show in this paper.

For not too large $|q|$, one expects that

$$\tau(q) = \tilde{\tau}(q), \quad (1.4)$$

which is the case when the IPR P_q represents a self-averaging quantity [see Subsection (III C) for a review]. At sufficiently large $|q|$, however, P_q becomes broadly distributed,^{2,12,15,22,23,28} and the corresponding $\tilde{\tau}(q)$ spectrum, dominated now by “rare events” induced by the disorder averaging procedure, deviates from $\tau(q)$.²⁹ While $\tilde{\tau}(q)$ is always easier to evaluate analytically, it is $\tau(q)$ that is most easily obtained from a representative wavefunction in numerics.^{4,5} By comparison, the *average* $\tilde{\tau}(q)$ and $\tilde{f}(\alpha)$ spectra were computed only recently via numerics at the IQHP¹⁶ and Anderson^{17,21} transitions.³¹

In this paper we calculate the typical multifractal spectrum at the Anderson MIT in the unitary¹ [broken time-reversal] symmetry class of disordered, normal metals, in $d > 2$. The spectrum $\tilde{\tau}(q)$ associated to the averaged IPR, evaluated at the metal-insulator transition in $d = 2 + \epsilon$, was obtained long ago^{8,32,33,34} via standard perturbative renormalization group (RG). The form of the *typical* $\tau(q)$ has been argued before only on heuristic grounds.^{3,23} We compute here for the first time the typical spectrum directly, using an (analytical) functional renormalization group (FRG) scheme^{25,26,27} previously employed in the study of wavefunctions statistics in a special class of disordered Dirac fermion models in 2D.^{22,24,25,26,27,35,36,37,38,39,40,41}

A. Average vs. typical spectra and termination

In the field theory description of Anderson localization [especially the non-linear sigma model (NL σ M) formulation,^{1,42} reviewed in Sec. II] the exponent $\tilde{\tau}(q)$, $q \in \mathbb{N}$ of the averaged IPR can be read off from the scaling dimensions x_q^* and x_1^* of local composite operators $\mathcal{O}_q(\mathbf{r})$ and $\mathcal{O}_1(\mathbf{r})$, which represent the q^{th} and 1^{st} moments of the local density of states (LDOS), respectively:^{8,43,44}

$$\tilde{\tau}(q) = d(q-1) + x_q^* - q x_1^*. \quad (1.5)$$

(See Sec. II for details.) For example, at the Anderson metal-insulator transition in $d = 2 + \epsilon$ dimensions in the unitary symmetry class, one obtains^{32,33,34}

$$x_q^* = -\Xi q(q-1) + \mathcal{O}[\epsilon^2 q^2 (q-1)^2], \quad (1.6a)$$

$$x_1^* = 0, \quad (1.6b)$$

$$\Xi = \sqrt{\epsilon/2} + \mathcal{O}(\epsilon^{5/2}). \quad (1.6c)$$

We can define a corresponding *average* singularity spectrum via

$$\begin{aligned} \tilde{f}(\alpha) &\equiv q\alpha - \tilde{\tau}(q), \quad \frac{d\tilde{\tau}(q)}{dq} = \alpha, \\ &= d - \tilde{f}_2 (\alpha - \alpha_0)^2 + \mathcal{O}[\sqrt{\epsilon}(\alpha - \alpha_0)^3], \end{aligned} \quad (1.7)$$

where

$$\tilde{f}_2 = \frac{1}{4\Xi} + \mathcal{O}(\epsilon), \quad (1.8a)$$

$$\alpha_0 = d + \Xi + \mathcal{O}(\epsilon^{5/2}). \quad (1.8b)$$

The corrections to [$\mathcal{O}(\dots)$ terms in] Eqs. (1.6a), (1.6c), and (1.7)–(1.8b) obtain at the fourth loop order³⁴ (or beyond) in the epsilon expansion. By contrast, Eq. (1.6b) is exact, and is equivalent to the statement that the average (global) density of states is non-critical at the MIT in the unitary symmetry class.^{45,46,47} In the present paper, we work only to the lowest non-trivial order in the expansion parameter $\sqrt{\epsilon}$. The consistency of the ϵ -expansion

in dealing with high moments of the LDOS operator is demonstrated in Sec. IV. Results similar to Eqs. (1.6a)–(1.6c) were first computed for the time-reversal invariant orthogonal^{8,49} symmetry class. The so-obtained $\tilde{f}(\alpha)$ spectrum is consistent with large-scale numerics.¹⁷

If one were to reconstruct the probability distribution of the wavefunction amplitudes from the average spectra [Eqs. (1.5) and (1.7)], a quadratic α -dependence of $\tilde{f}(\alpha)$ implies log-normal asymptotics of the distribution function.^{43,44,50,51,52} The precursor of this broad distribution is already visible at the crossover from the ballistic to diffusive regime, where wavefunctions start to show (weak) Anderson localization.¹ In this “pre-localized” regime, renormalization group studies of an (extended) NL σ M,^{43,44} as well as semi-classical analyses of the supersymmetric (SUSY) NL σ M^{50,51,52} predict that the distribution of the wavefunction amplitudes starts to deviate from the Gaussian, developing a log-normal tail.^{6,44} As it obtains from the $\tilde{\tau}(q)$ spectrum associated with the average of the IPR,^{43,44} this tail reflects the influence of rare realizations of the disorder and so-called “anomalously localized states.”^{50,51,52} Even though the tail of the distribution is still small, describing rare events in the mesoscopic regime, it is responsible for anomalous current relaxation, which is slower than expected from the Drude formula.^{44,50}

For small $\sqrt{\epsilon}$ (i.e., weak disorder) and q not too large, one might be inclined to expect that the results for $\tilde{\tau}(q)$ and $\tilde{f}(\alpha)$ in Eqs. (1.5)–(1.8b) should not differ substantially from $\tau(q)$ and $f(\alpha)$, respectively. However, the range of applicability of Eq. (1.7) to the typical $f(\alpha)$ is limited to $\alpha_- \leq \alpha \leq \alpha_+$, where, to lowest order

$$\alpha_{\pm} \equiv \left(\sqrt{d} \pm \sqrt{\Xi} \right)^2 + \dots, \quad (1.9)$$

so that $f(\alpha_{\pm}) = 0$. For $\alpha > \alpha_+$ and $\alpha < \alpha_-$, the average singularity spectrum $\tilde{f}(\alpha)$ becomes negative, which does not make sense if it is interpreted for a typical wavefunction [see the discussion following Eq. (1.2), above]. These thresholds define the critical values q_c^{\pm} of q for the $\tau(q)$ spectrum through

$$\begin{aligned} q_c^{\pm} &\equiv \frac{d\tilde{f}(\alpha_{\mp})}{d\alpha} = \pm q_c + \dots, \\ q_c &= \sqrt{\frac{d}{\Xi}}. \end{aligned} \quad (1.10)$$

For $q > q_c^+$, $q < q_c^-$, the typical spectrum $\tau(q)$ deviates completely from the average $\tilde{\tau}(q)$, given by Eqs. (1.5)–(1.6c) to lowest order in the epsilon expansion. Indeed, it can be rigorously proved⁴ that the $\tau(q)$ spectrum (as defined for a typical wavefunction) must be a monotonically increasing function of q ; by comparison, the average spectrum $\tilde{\tau}(q)$ in Eqs. (1.5)–(1.6c) is monotonically *decreasing* for $q > (d+\Xi)/2\Xi$. For $q > q_c^+$, $q < q_c^-$, the rare maxima (minima) of the wavefunction amplitude dominate the IPR [Eq. (1.1)], as computed for a representative wavefunction in a fixed disorder realization. In this

regime, the associated $\tau(q)$ is *linear* in q . By contrast, Eq. (1.4) holds for $q_c^- < q < q_c^+$. In Fig. 1, we plot the average spectrum $\tilde{\tau}(q)$ as given by Eqs. (1.5)–(1.6c), as well as our final result for the typical spectrum $\tau(q)$, which we obtain in Sec. III of this paper [Eq. (3.24), below].

We say that the multifractal behavior of the typical $\tau(q)$ spectrum “terminates” at $q = q_c^{\pm}$. This result in turn implies that the singularity spectrum $f(\alpha)$ must also suffer “termination,” i.e., vanish outside of the range bounded by α_{\pm} . The paramount distinction between typical vs. average spectra is therefore summarized as follows: the termination of $\tau(q)$ and $f(\alpha)$ reflects the dominance of *rare amplitude extrema* occurring in a representative wavefunction computed for a particular configuration of the disorder, whereas the deviation of $\tilde{\tau}(q)$ and $\tilde{f}(\alpha)$ from the former reflects the influence of *rare disorder realizations* that enter into the averaged IPR, \overline{P}_q [Eq. (1.3b)].

B. Operator product expansion and the functional renormalization group

The dimension x_q^* ($q \in \{1, 2, \dots\}$) in Eqs. (1.5) and (1.6a) describes the scaling of the disorder-averaged q^{th} LDOS moment at criticality, represented by the operator $\mathcal{O}_q(\mathbf{r})$. In order to extract the evolution of the typical value of an LDOS moment, we require a scaling equation for its entire probability distribution: a functional RG approach will turn out to be necessary. We will demonstrate that the scaling of the typical LDOS moments determines the $\tau(q)$ spectrum.

A key technical difference distinguishing the calculation of the typical $\tau(q)$ spectrum from that of the average $\tilde{\tau}(q)$ spectrum is that different LDOS moments couple to each other along the FRG flow. This coupling among the moments is encoded in the operator product expansion (OPE) of the scaling operators at the delocalization critical point,

$$\mathcal{O}_q(\mathbf{r}) \mathcal{O}_{q'}(\mathbf{r}') = \frac{C_{q,q'}^{q+q'}}{|\mathbf{r} - \mathbf{r}'|^{x_q^* + x_{q'}^* - x_{q+q'}^*}} \mathcal{O}_{q+q'}\left(\frac{\mathbf{r} + \mathbf{r}'}{2}\right) + \dots \quad (1.11)$$

Whenever the OPE coefficient $C_{q,q'}^{q+q'} \neq 0$, lower moments generate higher ones upon the RG transformation. The $\{x_q^*\}$ satisfy the convexity relation⁵³

$$x_{q+q'}^* < x_q^* + x_{q'}^* < 0 \quad (1.12)$$

for $q, q' > 1$. Since the $\{x_q^*\}$ are negative here, Eq. (1.12) indicates that higher moments are much more relevant, and hence we are forced to retain all mutually coupled moments in the theory, without being able to resort to truncation. The FRG allows us to organize and track the entire infinite tower of LDOS moment operators. The non-zero OPE coefficient $C_{q,q'}^{q+q'}$ leads to a non-linearity within the FRG; the unbounded broadening suggested by the q -dependence of x_q^* (reflecting the ever more relevant

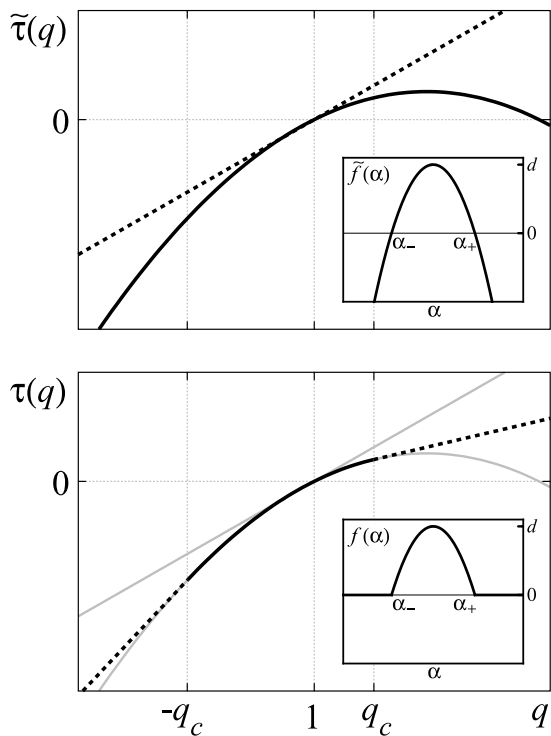


FIG. 1: Sketch of the multifractal spectra at the unitary class Anderson MIT. In the top panel, the heavy solid line corresponds to the average spectrum $\tilde{\tau}(q)$, defined by Eq. (1.3b) in the text, as obtained at the lowest non-trivial order in the ϵ -expansion [Eqs. (1.5)–(1.6c)].^{32,33,34} For comparison, the heavy dashed line in the same plot is the linear spectrum for a plane wave state, $\tilde{\tau}(q) = \tau(q) = d(q-1)$. In the bottom panel, the solid and dashed heavy line segments represent the typical spectrum $\tau(q)$, defined by Eq. (1.3a), as obtained in this paper via the functional renormalization group [see Eq. (3.24)]. For $q_c^- \leq q \leq q_c^+$ (solid segment of the curve in the bottom panel), the typical and average spectra coincide. By contrast, the typical spectrum is linear for $q < q_c^-$, $q > q_c^+$ (beyond “termination”), as depicted by the dashed curve segments in the bottom panel. The two curves in the top panel are rendered as faint gray lines in the bottom, for comparison. The inset in the top (bottom) panel depicts the average (typical) singularity spectrum at the unitary class MIT corresponding to the as-sketched $\tilde{\tau}(q)$ [$\tau(q)$].

nature of the corresponding operators, with increasing q) is balanced by this non-linearity. For small enough values of q , the non-linearity will entirely offset the unbounded broadening and render it inconsequential, whereas for sufficiently large values of q this will result in the termination of the typical $\tau(q)$ spectrum.

The mechanism described above is known to be responsible for the termination of the multifractal spectrum in a special (so-called ‘chiral’)⁴⁸ symmetry class of 2D models, possessing quenched disorder. Carpentier and Le Doussal^{25,26} pioneered the use of the FRG technique in their study of the random phase XY (gauge glass) model. This method was later applied²⁶ to the problem³⁵ of a 2D massless Dirac fermion, subject to a static, ran-

dom Abelian vector potential. The FRG provided direct confirmation of the multifractal termination for this problem, a result previously conjectured^{22,37} for the vector potential model. Later, Mudry et al.²⁷ extended the FRG to a more general 2D disordered Dirac model belonging to the symmetry class *BDI* (chiral orthogonal symmetry class). [We have adopted the nomenclature for quantum disorder classes employed in Ref. 48.] In these works, the FRG equation constructed from the set of operator scaling dimensions x_q^* and OPE coefficients $C_{q,q'}^{q+q'}$ [Eq. (1.11)] takes the form of the so-called Kolmogorov-Petrovsky-Piscounov (KPP) equation,⁵⁴ which describes non-linear diffusion in one dimension. It is the non-trivial behavior of the long-time asymptotics of the solution to the KPP equation that is responsible for the termination. We will show that the same equation arises in the general context of the typical $\tau(q)$ spectrum in the unitary symmetry class, at the Anderson MIT critical point in $d = 2 + \epsilon$ (with obvious extensions to additional symmetry classes).

C. Outline

Using the framework of the fermionic replica (compact) $NL\sigma M$ approach,^{1,42,55} we compute the OPE coefficient $C_{q,q'}^{q+q'}$ at the critical point in $d = 2 + \epsilon$ for the unitary class. Combining this result with the scaling dimensions given by Eqs. (1.6a)–(1.6c), we formulate the functional renormalization group for the tower of LDOS moment operators that enters into the computation of the typical $\tau(q)$ spectrum. Then we use the FRG to demonstrate that the same mechanism active in the 2D Dirac models,^{25,26,27} discussed above, leads to the termination of the multifractal spectrum at the MIT. We obtain the $\tau(q)$ spectrum for a typical wavefunction, which agrees with previous heuristic arguments.^{15,23}

The rest of the paper is organized as follows:

In Sec. II, we review the connection between the IPR and the local density of states, and we introduce a generating function that will be used to determine the typical $\tau(q)$ spectrum. We then establish conventions for the fermionic replica $NL\sigma M$, and identify the composite operators that represent moments of the local density of states in the low-energy field theory. In Sec. III we use the operator product expansion (OPE) of the LDOS moment operators at the MIT as input into the FRG, which then allows us to compute the scaling behavior of the generating function introduced in Sec. II. We thereby obtain the typical $\tau(q)$ spectrum. We discuss our results and draw conclusions in Sec. IV.

The derivation of the OPE of the operators $\{\mathcal{O}_q(\mathbf{r})\}$ representing the LDOS moments, which constitutes the technical field theoretic content of this work, has been relegated to Sec. V. In this Section, we rederive the anomalous scaling dimensions of the LDOS moment operators, and we compute the required OPE coefficient between properly normalized versions of these. The results ob-

tained are invoked as needed in the earlier Sec. III, so the reader less interested in calculational details may skip Sec. V entirely.

II. DEFINITIONS AND MODEL

A. Extracting multifractality from the LDOS – typical spectra

Consider the local density of states (LDOS), defined as

$$\begin{aligned} \nu(\varepsilon, \mathbf{r}) &= \frac{-1}{\pi} \text{Im} G_R(\varepsilon; \mathbf{r}, \mathbf{r}) \\ &= \sum_i \delta(\varepsilon - \varepsilon_i) |\psi_i(\mathbf{r})|^2, \end{aligned} \quad (2.1)$$

where the retarded Green's function is given by

$$G_R(\varepsilon; \mathbf{r}, \mathbf{r}') = \sum_i \frac{\psi_i(\mathbf{r}) \psi_i^*(\mathbf{r}')}{\varepsilon - \varepsilon_i + i\eta}, \quad (2.2)$$

with $\eta \rightarrow 0^+$.

On the metallic side of the delocalization transition, we cannot relate $P_q(\varepsilon)$, defined in terms of a single wavefunction by Eq. (1.1), directly to the LDOS.⁸ In order to use the field theory approach, we require that the LDOS constitute a smooth, well-defined function of energy in a closed, finite-size system; this necessitates the retention of the finite energy level broadening $\eta \gtrsim \Delta$, where Δ is the global level spacing. (Although a formal device in this context, the broadening may be attributed to, e.g., inelastic relaxation processes neglected in the non-interacting, single particle approach.)

We define⁸

$$\frac{1}{L^{d(q-1)} p^{(q)}(\varepsilon)} \equiv \frac{\int d^d \mathbf{r} \nu^q(\varepsilon, \mathbf{r})}{\left[\int d^d \mathbf{r} \nu(\varepsilon, \mathbf{r}) \right]^q}. \quad (2.3)$$

The quantity $p^{(q)}(\varepsilon)$ denotes the participation ratio, which receives contributions from states with energies residing in a window of width η about ε . On the metallic side of the transition, the right-hand side (RHS) of Eq. (2.3) should scale identically as Eq. (1.1).⁸

It will prove useful to introduce the moment generating function for the q^{th} power of the LDOS,

$$F_q(\xi; L) \equiv \left\langle \exp \left[-\xi \int d^d \mathbf{r} \nu^q(\varepsilon, \mathbf{r}) \right] \right\rangle, \quad (2.4)$$

where the angle brackets $\langle \dots \rangle$ denote a suitable ensemble average over realizations of the quenched disorder; L is the linear system size. Using the identity

$$\ln \phi = \int_0^\infty \frac{d\xi}{\xi} (e^{-\xi} - e^{-\phi\xi}) \quad (2.5)$$

and replacing P_q with the RHS of Eq. (2.3) in Eq. (1.3a), the typical multifractal spectrum exponent $\tau(q)$ may be written as

$$\tau(q) = \frac{d}{d \ln L} \int_0^\infty \frac{d\xi}{\xi} [F_q(\xi; L) - q F_1(\xi; L)]. \quad (2.6)$$

Our goal is to compute the scaling behavior of the moment generating function $F_q(\xi; L)$, and thereby obtain the typical $\tau(q)$ spectrum via Eq. (2.6). In closing this subsection, we note that the evaluation of Eq. (2.6) using the lowest order cumulant expansion for $F_q(\xi; L)$ recovers the average $\tilde{\tau}(q)$ spectrum, Eq. (1.5); we will discuss this point in detail in Sec. III.

B. NL σ M formulation

We examine in this paper the properties of the multifractal spectrum at the Anderson MIT in the unitary symmetry class. The critical point itself is accessed via the standard perturbative ϵ -expansion in $d = 2 + \epsilon$ dimensions, with $0 < \epsilon \ll 1$. Our low-energy, effective field theory starting point is the *compact* replica NL σ M,^{1,42,55} defined by the functional integral

$$Z \equiv \int \mathcal{D}[\hat{Q}] e^{-S},$$

where

$$S[\hat{Q}] \equiv \frac{1}{2t} \int d^d \mathbf{r} \text{Tr} \left(\nabla \hat{Q} \cdot \nabla \hat{Q} \right) - h \int d^d \mathbf{r} \text{Tr} \left(\hat{\Lambda}_z \hat{Q} \right). \quad (2.7)$$

In this equation, the “temperature” t is inversely proportional to the dimensionless dc conductance of the disordered metal, while the “external field” h serves as an infrared regulator, coupling to the local density of states (LDOS) operator, as defined below. The symbol \hat{Q} denotes a $2n \times 2n$ Hermitian matrix field satisfying

$$\hat{Q}^2(\mathbf{r}) = \hat{\mathbb{1}}_{2n}, \quad \text{Tr} \hat{Q}(\mathbf{r}) = 0. \quad (2.8)$$

The constant matrix

$$\hat{\Lambda}_z = \text{diag} \left(\hat{\mathbb{1}}_n, -\hat{\mathbb{1}}_n \right) \quad (2.9)$$

sets the (trivial) saddle-point for the action defined by Eq. (2.7). The identity in the space of $2n \times 2n$ and $n \times n$ square matrices is denoted by $\hat{\mathbb{1}}_{2n}$ and $\hat{\mathbb{1}}_n$ in Eqs. (2.8) and (2.9), respectively. In these equations, n is proportional to the number of replicas, with $n \rightarrow 0$ at the end of the calculation.^{1,42} The target space of the NL σ M is the compact coset $G(2n)/G(n) \times G(n)$, where $G = O, U, Sp$ for the orthogonal, unitary, and symplectic symmetry classes, respectively. In the following, we focus upon the unitary universality class, $G = U$. The field theory in Eqs. (2.7) and (2.8) can be derived⁵⁵ from a microscopic Grassmann path integral describing a system

of non-interacting fermions, lacking time-reversal invariance, averaged over configurations of a Gaussian, white noise-correlated random potential.

We employ ‘ σ - π ’ coordinates⁴⁶ on the target manifold,

$$\hat{Q} = \begin{bmatrix} (\hat{\mathbb{I}}_n - \hat{W}\hat{W}^\dagger)^{1/2} & \hat{W} \\ \hat{W}^\dagger & -(\hat{\mathbb{I}}_n - \hat{W}^\dagger\hat{W})^{1/2} \end{bmatrix}. \quad (2.10)$$

For the unitary class, $\hat{W}(\mathbf{r}) \rightarrow W^\alpha_\beta(\mathbf{r})$ is an unconstrained, complex-valued matrix, with $\alpha, \beta \in \{1, \dots, n\}$.

Non-interacting electrons residing in $d > 2$ spatial dimensions and subject to quenched disorder possess a diffusive metallic phase, defined as the presence of extended wavefunctions at the Fermi energy, provided that the disorder is sufficiently weak. The disorder strength is quantified by the “bare” conductance at the scale of the mean free path, proportional to $1/t$ in the effective field theory [Eq. (2.7)]. In direct analogy with the $O(3)/O(2)$ NL σ M description of classical magnetic ordering,^{56,57,58} the “low temperature” (weak disorder) regime $0 \leq t < t^*$ of the model in Eq. (2.7) exhibits spontaneous continuous symmetry breaking, so that the ‘ σ ’ fields $(\hat{\mathbb{I}}_n - \hat{W}\hat{W}^\dagger)^{1/2}$ and $(\hat{\mathbb{I}}_n - \hat{W}^\dagger\hat{W})^{1/2}$, which form the diagonal elements of the \hat{Q} -matrix in the parameterization of Eq. (2.10), acquire non-zero expectation values throughout the diffusive metallic phase. By contrast, the off-diagonal ‘ π ’ fields \hat{W} and \hat{W}^\dagger represent small spatial fluctuations with vanishing mean in this regime. Here, $t = t^* > 0$ locates the MIT in $d = 2 + \epsilon$.

An unusual aspect of the theory of the MIT transcribed in Eq. (2.7) is the fact that this spontaneous symmetry breaking occurs also at the delocalization transition itself ($t = t^*$), and survives even into the insulating (“high temperature”) phase ($t > t^*$).^{45,46} In the effective NL σ M field theory, the trace of the matrix $\hat{\Lambda}_z \hat{Q}(\mathbf{r})$ represents the LDOS $\nu(\epsilon, \mathbf{r})$ [Eq. (2.1)] for the disordered electron system:⁸

$$\begin{aligned} \nu(\epsilon, \mathbf{r}) &\sim \text{Tr} \left[\hat{\Lambda}_z \hat{Q}(\mathbf{r}) \right] \\ &= \text{Tr} \left\{ \left[\hat{\mathbb{I}}_n - \hat{W}\hat{W}^\dagger(\mathbf{r}) \right]^{1/2} + \left[\hat{\mathbb{I}}_n - \hat{W}^\dagger\hat{W}(\mathbf{r}) \right]^{1/2} \right\}. \end{aligned} \quad (2.11)$$

This is the same operator that appears in the action Eq. (2.7), where it couples to the external field parameter h . While the *character* of the typical wavefunction changes from extended to localized upon traversing the mobility edge, as encoded by, e.g., the typical multifractal exponent $\tau(q)$ for $q \geq 2$ [Eq. (2.6)], the average density of states does not exhibit critical behavior across the transition.⁴⁵ The LDOS operator on the RHS of Eq. (2.11) retains a non-zero expectation value so long as the average density of states is non-vanishing; consequently, the \hat{Q} -matrix cannot be interpreted as an order parameter for the MIT. Technically, this result (an exception to Goldstone’s theorem)⁴⁶ obtains from the NL σ M only *after* the replica limit $n \rightarrow 0$ is taken.

For any non-zero, integral number of replicas $n \in \{1, 2, \dots\}$, the model in Eq. (2.7) also possesses a (different) second order transition at $t = t_n^* > 0$, separating a low temperature “ferromagnetic” phase ($t < t_n^*$) from the high temperature “paramagnet” ($t > t_n^*$). In contrast to the replica limit $n \rightarrow 0$ appropriate to the description of electronic wavefunction (de)localization, the NL σ M with $n \geq 1$ is characterized by a *restoration* of the symmetry at the critical point between the ‘ σ ’ (diagonal) and ‘ π ’ (off-diagonal) components of the \hat{Q} -matrix, within the parameterization given by Eq. (2.10). This is the conventional behavior expected for a classical statistical mechanics model describing spontaneous continuous symmetry breaking in the vicinity of the critical point.

Let us assume that we are interested only in properties of the NL σ M given by Eq. (2.7) at the critical point, $t = t_n^*$. Because the symmetry is restored at the transition, for non-zero n we are permitted to make the following $U(2n)$ “rotation” from $\hat{\Lambda}_z$ to $\hat{\Lambda}_x$ in Eq. (2.11):

$$\begin{aligned} \nu(\epsilon, \mathbf{r}) &\sim \text{Tr} \left[\hat{\Lambda}_z \hat{Q}(\mathbf{r}) \right] \rightarrow \text{Tr} \left[\hat{\Lambda}_x \hat{Q}(\mathbf{r}) \right] \\ &= \text{Tr} \left[\hat{W}(\mathbf{r}) + \hat{W}^\dagger(\mathbf{r}) \right], \end{aligned} \quad (2.12)$$

where $\hat{\Lambda}_x$ denotes the block Pauli matrix generalizing Eq. (2.9), in the standard basis.

In the technical field theoretic portion of this paper, Sec. V, we employ the NL σ M defined by Eqs. (2.7)–(2.10) to extract the properties of the LDOS operator and its moments. Our strategy is to work, as usual, at fixed, integral $n \geq 1$ throughout the intermediate stages of our computations. At the critical point in $d = 2 + \epsilon$, we are then free to employ the LDOS representation given by the RHS of Eq. (2.12). Only at the end of our work will we perform the required analytic continuation $n \rightarrow 0$ (which smoothly deforms $t_n^* \rightarrow t^*$), so as to obtain (perturbative) results appropriate to the MIT.

C. LDOS moments as composite eigenoperators

Higher integral moments of the LDOS can be similarly represented by local composite operators in the NL σ M. The renormalization group (RG) transformation does not preserve the form of an operator

$$\nu^p = \left[\text{Tr} \left(\hat{W} + \hat{W}^\dagger \right) \right]^p, \quad (2.13)$$

obtained by taking a power of Eq. (2.12). Nevertheless, such a structure can be decomposed into invariant eigenoperators, each of which possessing an independent scaling dimension.

This idea is most easily understood via analogy to the simpler $O(3)/O(2)$ model,^{56,57,58} to which the field theory defined by Eqs. (2.7)–(2.10) reduces for the case of $n = 1$ [since $U(2)/U(1) \times U(1) \sim SU(2)/U(1) \sim O(3)/O(2)$]. In this NL σ M, the target manifold is simply the two-sphere, parameterized by the unconstrained

transverse coordinates $\pi_{\pm} \equiv \pi_x \pm i\pi_y$, with z -component $\sigma = \sqrt{1 - \pi_+ \pi_-}$. A complete basis of local eigenoperators with no derivatives is the set of ordinary spherical harmonics $\{Y_{l,m}(\pi_+, \pi_-, \sigma)\}$. All operators belonging to a given irreducible representation of the symmetry group possess the same renormalization; therefore, any linear combination of spherical harmonics sharing a common l value constitutes an eigenoperator. The field coordinates π_{\pm} are themselves eigenoperators belonging to $l = 1$, as is the combination

$$\nu \equiv \pi_+ + \pi_- \propto Y_{1,-1} - Y_{1,1}. \quad (2.14)$$

For an arbitrary integer moment of ν , one can use angular momentum addition to establish the decomposition

$$(\pi_+ + \pi_-)^l = \sum_{j=0}^l \mathcal{O}_j^{(l)}, \quad (2.15)$$

where the eigenoperators $\mathcal{O}_j^{(l)}$ are defined via

$$\mathcal{O}_j^{(l)} = \sum_{m=-j}^j \kappa_{j,m}^{(l)} Y_{j,m}(\pi_+, \pi_-, \sigma). \quad (2.16)$$

with certain coefficients $\kappa_{j,m}^{(l)}$. For the highest total angular momentum block $j = l$ in Eq. (2.15), one has

$$\mathcal{O}_l^{(l)} = (\pi_-^l + \dots + \pi_+^l), \quad (2.17)$$

since the ‘‘highest and lowest weight states’’ π_+^l and π_-^l are eigenoperators proportional to $Y_{l,l}$ and $Y_{l,-l}$, respectively.

The coefficients $\{\kappa_{j,m}^{(l)}\}$ on the RHS of Eq. (2.16) are determined entirely by group theory (i.e., are composed of sums of products of appropriate Clebsch-Gordan coefficients),⁵⁹ up to an overall m -independent normalization for all operators belonging to a given total angular momentum block j . This normalization can be established via the convention

$$Y_{l,-l} \equiv \lambda_l \pi_-^l. \quad (2.18)$$

In a similar fashion, the operator in Eq. (2.13) should be decomposed into a sum of terms belonging to different irreducible representations of the group $U(2n)$. Each such term can be further decomposed into a linear combination of basis operators with appropriate ‘‘magnetic’’ quantum numbers determined by the transformation properties under the subgroup $U(n) \times U(n)$.

It is useful to push this analogy a little further. In order to extract the typical $\tau(q)$ spectrum in the unitary class model, we need the scaling dimension of the most relevant eigenoperator (in the RG sense) contributing to each of the p^{th} LDOS moments in Eq. (2.13), $p \in \{1, 2, \dots\}$, as well as the operator product expansion (OPE) between pairs of such most relevant eigenoperators. The most relevant eigenoperator contributing to

the decomposition of Eq. (2.13), for a given fixed p , is analogous to the highest (total) angular momentum operator $\mathcal{O}_l^{(l)}$ contributing to the l^{th} moment of $(\pi_+ + \pi_-)$ in Eq. (2.15),⁶⁰ with $l = p$. [Precise definitions of the eigenoperators that we employ in the $U(2n)/U(n) \times U(n)$ NL σ M are given by Eqs. (2.23) and (2.24), below.] In the $O(3)/O(2)$ model, we can effectively trade the operator $\mathcal{O}_l^{(l)}$, which for large l is a complicated sum of many terms according to Eq. (2.16), for its lone ‘‘lowest weight state’’ component $Y_{l,-l}$ [Eqs. (2.17) and (2.18)]. Obviously, both operators share the same scaling dimension. Moreover, the structure of the OPE between $\mathcal{O}_l^{(l)}$ and $\mathcal{O}_{l'}^{(l')}$ follows from that of the product between their lowest weight state constituents. Consider the following OPE at zero coupling ($t = 0$):

$$\begin{aligned} \lambda_l \lambda_{l'} \mathcal{O}_l^{(l)} \mathcal{O}_{l'}^{(l')} &= c_{l,l'}^{l+l'} \lambda_{l+l'} \mathcal{O}_{l+l'}^{(l+l')}, \\ (Y_{l,-l} + \dots)(Y_{l',-l'} + \dots) &= c_{l,l'}^{l+l'} (Y_{l+l',-l-l'} + \dots), \end{aligned} \quad (2.19)$$

where we have defined the OPE coefficient

$$c_{l,l'}^{l+l'} \equiv \frac{\lambda_l \lambda_{l'}}{\lambda_{l+l'}}. \quad (2.20)$$

The crucial point is that the relative weight of each term appearing in the expansion for the eigenoperator $\mathcal{O}_l^{(l)}$ [Eq. (2.16)] is entirely fixed by group theory; only the overall, l -dependent normalization is arbitrary. The required OPE coefficient in Eq. (2.20) is then determined by just this normalization for the lowest weight state operators, Eq. (2.18). Of course, this argument neglects loop corrections, which may modify the value of the OPE coefficient given by Eq. (2.20), computable systematically within the ϵ -expansion. This, however, cannot alter the structure of Eq. (2.19).

With the above in mind, we consider the component

$$[\text{Tr } \hat{W}]^p \quad (2.21)$$

of the LDOS moment in Eq. (2.13). As opposed to the sphere model discussed above, this pure \hat{W} power does not represent an eigenoperator for $n > 1$. However, a useful subset⁶¹ of the RG eigenoperators *can* be built out of p -fold products of ‘ π ’ ($W^{\alpha\beta}$) field matrix elements:

$$\mathcal{O}_{p \text{ } (\beta_1 \beta_2 \dots \beta_p)_{\mathcal{Y}}}^{\alpha_1 \alpha_2 \dots \alpha_p}(\mathbf{r}) \equiv \frac{1}{p!} W^{\alpha_1}_{\beta_1} W^{\alpha_2}_{\beta_2} \dots W^{\alpha_p}_{\beta_p}, \quad (2.22)$$

where $(\dots)_{\mathcal{Y}}$ means a suitable symmetrization prescribed by a Young tableau \mathcal{Y} . For fixed p , the most relevant operator (in the sense of the RG, at the MIT in $d = 2 + \epsilon$) is given by the totally antisymmetric Young tableau,^{8,32}

$$\begin{aligned} \mathcal{O}_{p \text{ } [\beta_1 \beta_2 \dots \beta_p]}^{\alpha_1 \alpha_2 \dots \alpha_p}(\mathbf{r}) \\ \equiv \left(\frac{1}{p!}\right)^2 \sum_{\mathbf{P}} \text{sgn}(\mathbf{P}) [W^{\alpha_1}_{\beta_{\mathbf{P}(1)}} \dots W^{\alpha_p}_{\beta_{\mathbf{P}(p)}}], \end{aligned} \quad (2.23)$$

with \mathbf{P} a permutation of p symbols; $\text{sgn}(\mathbf{P})$ denotes the sign of the permutation. Because of the antisymmetrization requirement, each distinct operator defined through Eq. (2.23) is identified by any permutation of a complete set of indices $\{\alpha_i\}$ satisfying $\alpha_1 \neq \alpha_2 \neq \dots \neq \alpha_p$, and similarly for the $\{\beta_i\}$. Indices range from 1 to n , so that many different operators can be associated to each integral moment of the LDOS, at least for sufficiently large n .

Physically, we would like establish a one-to-one correspondence between the p^{th} LDOS moment $[\nu(\varepsilon, \mathbf{r})]^p$ in the disordered electron system, and a single, *unique* operator \mathcal{O}_p in the NL σ M field theory that represents its most relevant component. This can be accomplished by tracing over pairs of indices in Eq. (2.23) in the following fashion:

$$\mathcal{O}_p(\mathbf{r}) \equiv \sum_{\alpha_1=1}^n \dots \sum_{\alpha_p=1}^n \mathcal{O}_{p[\alpha_1\alpha_2\dots\alpha_p]}^{\alpha_1\alpha_2\dots\alpha_p}(\mathbf{r}). \quad (2.24)$$

With this definition, the eigenoperators

$$\mathcal{O}_2 = \frac{[\text{Tr}(\hat{W})]^2 - \text{Tr}(\hat{W}^2)}{(2!)^2},$$

$$\mathcal{O}_3 = \frac{[\text{Tr}(\hat{W})]^3 - 3 \text{Tr}(\hat{W}^2) \text{Tr}(\hat{W}) + 2 \text{Tr}(\hat{W}^3)}{(3!)^2},$$

etc., are easily recognized as natural deformations of the LDOS moments obtained by taking powers of Eq. (2.21).⁶¹ Moreover, we will establish in Sec. V that the set $\{\mathcal{O}_p\}$ closes under the operator product expansion (OPE), up to less relevant operators generated on the right-hand side of Eq. (1.11), which we may ignore. This is a sufficient condition to apply the functional renormalization group method.

In summary, the operators defined by Eqs. (2.23) or (2.24) constitute the most relevant component(s) of the p^{th} moment of the LDOS^{8,32,61} at the MIT, and hence dominate its scaling behavior there.

D. Augmented NL σ M

At the metal-insulator critical point, the scaling of the average IPR \overline{P}_q [i.e., the multifractal exponent $\tilde{\tau}(q)$, Eq. (1.3b)] can be extracted solely from the scaling dimensions x_p^* of the local composite operators $\mathcal{O}_{p[\beta_1\beta_2\dots\beta_p]}^{\alpha_1\alpha_2\dots\alpha_p}(\mathbf{r})$ or $\mathcal{O}_p(\mathbf{r})$, with $p \in \{1, q\}$ —this is the content of Eq. (1.5) in the Introduction. By contrast, the probability distribution functions of the IPR and LDOS [reflected by the typical multifractal exponent $\tau(q)$, Eq. (1.3a)] are described by the complicated generating function $F_q(\xi; L)$, introduced in Eq. (2.4). In the low-energy theory, $F_1(\xi; L)$ can be represented by the NL σ M in Eq. (2.7) with a bare non-zero external field parameter h_0 given by

$$h_0 = -\xi. \quad (2.25)$$

Performing a renormalization group transformation upon the NL σ M with $h_0 \neq 0$ generically produces higher powers of the LDOS operator as new perturbations to the action S , so that terms of the form

$$\delta S = -Y_m \int d^d \mathbf{r} \left\{ \text{Tr} \left[\hat{\Lambda}_z \hat{Q}(\mathbf{r}) \right] \right\}^m, \quad (2.26)$$

for example, will be generated. Here, Y_m is a coupling constant. The structure in Eq. (2.26) is not invariant under the RG; with further iterations, it will **(a)** mix with other terms sharing the same “engineering” dimension, and **(b)** fuse with other terms and with itself to produce new perturbations. Among the flood of structures that arise, we will focus only upon the most relevant terms that determine the leading scaling behavior for the generating function $F_1(\xi; L)$ of the LDOS and its moments.

Anticipating the generation of higher moments upon renormalization, we should augment the action in Eq. (2.7) (with $h_0 = 0$) by a term of the form

$$\delta S \equiv - \sum_{p=1}^{\infty} Y_p \int d^d \mathbf{r} \mathcal{O}_p(\mathbf{r}), \quad (2.27)$$

where the “traced” moment operators \mathcal{O}_p were defined above by Eq. (2.24).

At tree level, the operators defined by Eqs. (2.23) and (2.24) are dimensionless, so that the corresponding coupling constants $\{Y_p\}$ are strongly relevant perturbations to the NL σ M action. As discussed in Sec. I A, they prove even more relevant at the non-trivial fixed point (perturbatively accessible Anderson MIT). Moreover, the higher moments are more relevant compared to the lower ones [Eq. (1.12)]. The FRG approach tracks the scaling behavior of this entire tower of operators, and uses this data to make non-trivial predictions about observable statistics, such as the *typical* LDOS. Within the FRG framework, only two pieces of information are needed: first, the scaling dimensions of the operators in Eqs. (2.23) and (2.24), and second, the coefficient $C_{q,q'}^{q+q'}$ for the operator product $\mathcal{O}_q \otimes \mathcal{O}_{q'} \rightarrow \mathcal{O}_{q+q'}$, as defined by the OPE in Eq. (1.11). All quantities are to be evaluated at the MIT in $d = 2 + \epsilon$.

We use a two-stage approach to the renormalization of the “extended” NL σ M [the action Eq. (2.7) supplemented with (2.27)]. The idea is to first locate the non-trivial metal-insulator fixed point in $d = 2 + \epsilon$, obtained via the standard ϵ -expansion by renormalizing the theory in Eq. (2.7) with $h \rightarrow 0$. (We will use dimensional regularization.) We then compute the OPE [Eq. (1.11)] at the MIT to the lowest non-trivial order in $\sqrt{\epsilon}$. Finally, we run a ‘one-loop’ RG calculation *at this non-trivial fixed point*, for the full model defined by Eqs. (2.7) and (2.27). The required one-loop functional renormalization group equation is obtained from the OPE.⁶² Note that since we are interested in LDOS and IPR statistics at the Anderson metal-insulator transition ($t = t^*$), rather than in the diffusive metallic phase ($t < t^*$), we are required to run the FRG at this non-trivial fixed point.⁶³

In order to streamline the presentation, the above-described field theory calculations are relegated to the last Sec. V of this paper. The obtained results required for the functional RG are simply invoked as needed in the next Sec. III, so that the reader less interested in calculational details may avoid Sec. V entirely.

III. FUNCTIONAL RG FOR THE TYPICAL $\tau(q)$ SPECTRUM

A. From coupled RG to KPP equations

The typical $\tau(q)$ spectrum, defined in Sec. I by Eq. (1.3a), can be extracted from the generating function $F_q(\xi; L)$, introduced in Eq. (2.4). The relationship is expressed by Eq. (2.6). In terms of the NL σ M formulation reviewed in Secs. II B–II D, $F_q(\xi; L)$ may be encoded as

$$F_q(\xi; L) \sim \left\langle \exp \left[\sum_{p=1}^{\infty} Y_{pq} \int d^d \mathbf{r} [\mathcal{O}_{pq}](\mathbf{r}) \right] \right\rangle, \quad (3.1)$$

where $q = 1, 2, 3, \dots$, and $[\mathcal{O}_{pq}](\mathbf{r})$ is a “renormalized and normalized” LDOS moment eigenoperator, defined by Eq. (5.35) in the technical Sec. V of this paper. [Note that here pq denotes the product of the integers p and q . $[\mathcal{O}_m](\mathbf{r})$ is just a normalized version of the LDOS moment operator $\mathcal{O}_m(\mathbf{r})$, defined previously via Eq. (2.24). The careful normalization of operators is an important technical step required for the accurate computation of correlation functions at the MIT, as detailed in Sec. V. In this Section, we merely assert that the proper procedure has been implemented.] Eq. (3.1) generalizes Eq. (2.27) for the case of $q > 1$: in order to compute $F_q(\xi; L)$, one must augment the bare sigma model action with the operator tower $\{[\mathcal{O}_q], [\mathcal{O}_{2q}], [\mathcal{O}_{3q}], \dots\}$, since through the OPE operators representing lower integral LDOS moments generate new ones representing higher integral multiples of these. For $q > 1$, the operators in Eq. (3.1) form a *subset* of those in Eq. (2.27). The expectation $\langle \dots \rangle$ in Eq. (3.1) is taken with respect to the NL σ M action at the MIT in $d = 2 + \epsilon$, Eq. (2.7), with $h = 0$ and $t = t^*$. The coupling constants Y_{pq} take the bare values

$$Y_{pq}(l = 0) = -\xi \delta_{p,1}. \quad (3.2)$$

Here, $l = \ln L/L_0$ is the log of the spatial length scale L (e.g., the system size), with L_0 an arbitrary reference scale.

The simplest approximation to $F_q(\xi; L)$ obtains from the lowest order cumulant expansion of Eq. (3.1), evaluated at $L = L_0$ [i.e. using the bare coupling constants in Eq. (3.2)]:

$$\begin{aligned} F_q(\xi; L_0) &\sim \exp \left[-\xi \int d^d \mathbf{r} \langle [\mathcal{O}_q] \rangle \right] \\ &\sim \exp \left(-\xi L_0^{d-x_q^*} \right). \end{aligned} \quad (3.3)$$

In this equation, x_q^* denotes the negative scaling dimension of the operator $[\mathcal{O}_q](\mathbf{r})$ at the MIT; for the unitary class studied here, the result to lowest order in $\sqrt{\epsilon}$ was given by Eqs. (1.6a) and (1.6c), above. Combining Eqs. (3.3) and (2.6), we immediately recover Eq. (1.4): the lowest order cumulant approximation to $F_q(\xi; L_0)$ equates the *typical* $\tau(q)$ spectrum with $\tilde{\tau}(q)$ [Eqs. (1.5)–(1.6c)], associated to the average of the IPR. For sufficiently large moments with $q > q_c$, where q_c was defined by Eq. (1.10), this identification invariably breaks down (see the discussion in Sec. I A); an accurate computation of Eq. (3.3) then requires the retention of higher order cumulants. One immediately sees the need for the operator product expansion (OPE), as defined by Eq. (1.11): the second and higher cumulants involve products of LDOS moment operators, integrated over the sample volume. When two (or more) such operators approach the same spatial position, fusion can occur, in which new, higher moment operators are generated through short-distance regularization.^{25,26,27,58,62} At the MIT, the negative scaling dimensions $\{x_q^*\}$ of the LDOS moment operators [Eqs. (1.6a)–(1.6c)] satisfy the convexity relation given by Eq. (1.12). Therefore, operators corresponding to successively higher moments carry ever more negative scaling dimensions, contributing ever more strongly to the cumulant expansion.

Rather than compute the generating function $F_q(\xi; L)$ directly, we will use scaling arguments to extract its asymptotic behavior in the large system size limit, $L/L_0 \rightarrow \infty$. In Eq. (3.1), the LDOS moment operators $[\mathcal{O}_{pq}]$ perturb the action of the critical field theory. It is well known that the lowest order RG equations for the set of conjugate coupling constants Y_{pq} follow directly from the operator product expansion.⁶²

In Sec. V, we demonstrate that (the properly normalized versions of) the operators defined by Eq. (2.24) obey the OPE given by Eq. (1.11) at the MIT in $d = 2 + \epsilon$. We find that the OPE coefficient is given by the “tree level” (zero coupling) amplitude

$$C_{q,q'}^{q+q'} = \frac{(q+q')!}{q!q'!} + \mathcal{O}(\epsilon). \quad (3.4)$$

These results are obtained as Eqs. (5.33) and (5.34) in Sec. V, where we demonstrate that the lowest order $t^* \propto \sqrt{\epsilon}$ (one-loop) correction to the OPE coefficient in Eq. (3.4) vanishes. Using Eqs. (1.11) and (3.4), one finds the infinite set of RG equations⁶²

$$\frac{dY_{pq}}{dl} = (d-x_{pq}^*)Y_{pq} + \frac{S_d}{2} \sum_{m=1}^{p-1} \binom{p}{m} Y_{mq} Y_{(p-m)q} + \mathcal{O}(Y^3), \quad (3.5)$$

where S_d is the surface area of the sphere in d dimensions. Through the OPE, lower moment coupling constants always generate higher ones; the convexity property in Eq. (1.12) implies that, for $p > p'$, a non-zero Y_{pq} represents a much more relevant perturbation than $Y_{p'q}$ to the critical NL σ M action. Clearly we must retain the entire infinite set $\{Y_{pq}\}$ in our analysis.

At first glance, the generation of infinitely many relevant couplings would seem to imply non-universality: there are infinitely many classes of solutions to the RG equations (3.5), and hence there are infinitely many ways to depart from the RG fixed point representing the MIT. This is consistent with the fact that a random critical point should be characterized by the entire distribution functions of physical quantities, which can become very broad. At a delocalization critical point, however, the multifractal $\tau(q)$ and $f(\alpha)$ spectra, associated to a typical wavefunction in a fixed disorder realization, are both self-averaging^{15,23} and universal.^{5,14,16,18,19} We will demonstrate that the functional renormalization group (FRG) method gives a universal prediction for $\tau(q)$ and $f(\alpha)$, below and above termination (as defined in Sec. IA), at the unitary class Anderson MIT in $d = 2 + \epsilon$ consistent with this picture.

We can trade the coupled set of ordinary differential equations in Eq. (3.5) for a single partial differential equation (PDE) by defining the auxiliary generating function²⁷

$$G_q(z, l) \equiv \tilde{G}_q(\tilde{z}, \tilde{l}) \equiv 1 + \frac{S_d}{2d} \sum_{p=1}^{\infty} \frac{(e^{-z})^p}{p!} Y_{pq}(l), \quad (3.6)$$

where we have introduced the ‘‘position coordinate’’ z . $\tilde{G}_q(\tilde{z}, \tilde{l})$ is a ‘‘Galilean boost’’ of $G_q(z, l)$, with

$$\tilde{z} \equiv z + \Xi ql, \quad \tilde{l} \equiv l. \quad (3.7)$$

At the unitary class MIT in $d = 2 + \epsilon$, the parameter Ξ has the value given by Eq. (1.6c), to one-loop order.

Using the RG equations (3.5) for the coupling constants $\{Y_{pq}\}$, and the explicit form of x_{pq}^* from Eqs. (1.6a)–(1.6c), one can easily show that $\tilde{G}_q(\tilde{z}, \tilde{l})$ satisfies the following Kolmogorov-Petrovsky-Piscounov (KPP) equation:

$$\frac{1}{d} \partial_{\tilde{z}} \tilde{G}_q = D_q \partial_{\tilde{z}}^2 \tilde{G}_q + \tilde{G}_q (\tilde{G}_q - 1), \quad (3.8)$$

where we have introduced the effective diffusion constant

$$D_q \equiv \frac{q^2 \Xi}{d}. \quad (3.9)$$

The same Eq. (3.8) was obtained in previous FRG studies of 2D disordered systems.^{25,26,27}

B. Solution to the KPP equation and results

The KPP equation (3.8) describes non-linear diffusion phenomena. The positive D_q in Eq. (3.9) reflects the diffusion of the distribution function for the inverse participation ratio (IPR), defined by Eq. (1.1). For high moments, $q \gg 1$, this diffusion constant is very large, indicating that the IPR becomes broadly distributed in the large system size limit; in this regime, the $\tilde{\tau}(q)$ spectrum

associated with the average IPR [Eq. (1.3b)] is dominated by rare realizations of the disorder, and loses its meaning with respect to the typical wavefunction. The non-linear term in Eq. (3.8) appears because the generating functions $\tilde{G}_q(\tilde{z}, \tilde{l})$ and $F_q(\xi; L)$ encode information about the typical $\tau(q)$ spectrum; this non-linearity arises through the OPE between LDOS moment operators [Eqs. (1.11) and (3.4)]. As explained in the paragraph following Eq. (3.3), the OPE is the essential ingredient required in the computation of $\tau(q)$, which was missed in previous treatments^{8,43,44} of the Anderson MIT based upon the NL σ M approach.

Non-linear PDEs are often not analytically solvable, but a number of key results are known for the KPP equation. We summarize here only those features essential to the computation of $\tau(q)$; for further details, consult Refs. 25,26,27 and the references therein. For a large class of initial conditions which satisfy

$$\lim_{\tilde{z} \rightarrow +\infty} \tilde{G}_q(\tilde{z}, 0) = 1, \quad (3.10a)$$

$$\lim_{\tilde{z} \rightarrow -\infty} \tilde{G}_q(\tilde{z}, 0) = 0, \quad (3.10b)$$

$\tilde{G}_q(\tilde{z}, \tilde{l})$ converges to a stable traveling wave solution propagating in the positive \tilde{z} direction,

$$\tilde{G}_q(\tilde{z}, \tilde{l} \rightarrow \infty) \rightarrow h(\tilde{z} - \tilde{c}_q \tilde{l}), \quad (3.11)$$

where the constant \tilde{c}_q denotes the wavefront velocity. The functional form of the traveling wave in Eq. (3.11) is sensitive to the details of the initial condition at $\tilde{l} = 0$. On the contrary, for an initial wavefront satisfying the asymptotic property

$$\tilde{G}_q(\tilde{z} \rightarrow +\infty, 0) \sim 1 - \lambda e^{-\tilde{z}}, \quad (3.12)$$

with λ a pure number, the velocity \tilde{c}_q is *universal*, depending only upon the diffusion constant D_q , defined in the context of the MIT by Eq. (3.9), above. Note that Eq. (3.12) constrains \tilde{G}_q only in the region penetrated by the wavefront [Eq. (3.11)] in the limit of large ‘‘renormalization time,’’ $\tilde{l} \rightarrow \infty$. Remarkably, the wavefront velocity is also insensitive to the precise form of the non-linear term $\mathcal{F}(\tilde{G}_q) \equiv \tilde{G}_q(\tilde{G}_q - 1)$ in the KPP equation (3.8). In fact, the same velocity obtains from KPP for any nonlinear forcing function satisfying the constraints

$$\begin{aligned} \mathcal{F}(0) = \mathcal{F}(1) = 0, \quad \mathcal{F}(\tilde{G}) < 0, \\ \frac{d\mathcal{F}(\tilde{G})}{d\tilde{G}} \geq -1, \quad \frac{d\mathcal{F}(\tilde{0})}{d\tilde{G}} = -1, \end{aligned} \quad (3.13)$$

for $0 \leq \tilde{G} \leq 1$. In this sense, the KPP equation achieves a strong version of universality.

Let us now return to the problem at hand, computing the typical $\tau(q)$ spectrum obtained at the MIT in the unitary class for $d = 2 + \epsilon$. The initial condition for the KPP Eq. (3.8) implied by Eq. (3.2) is

$$\tilde{G}_q(\tilde{z}, 0) = 1 - \xi \frac{S_d}{2d} e^{-\tilde{z}}, \quad (3.14)$$

consistent with only Y_q non-vanishing. Eq. (3.14) satisfies the condition in Eq. (3.10a), having the same form as that expressed in Eq. (3.12). In order to satisfy Eq. (3.10b), we must bound the amplitude $0 \leq \tilde{G}_q(\tilde{z} \rightarrow -\infty, 0) \leq 1$; to that end, we deform Eq. (3.2) as follows:

$$\begin{aligned} Y_q(0) &= -\xi, \\ Y_{pq}(0) &\rightarrow \left(\frac{S_d}{2d}\right)^{p-1} [Y_q(0)]^p, \end{aligned} \quad (3.15)$$

which leads to

$$\tilde{G}_q(\tilde{z}, 0) \sim \exp\left[-\xi \frac{S_d}{2d} e^{-\tilde{z}}\right]. \quad (3.16)$$

Crucially, since Eq. (3.16) satisfies Eq. (3.12), the asymptotic traveling wave velocity \tilde{c}_q [Eq. (3.11)] depends only upon the diffusion constant D_q , Eq. (3.9). For the KPP equation (3.8) satisfying (3.10a), (3.10b), and (3.12), one finds qualitatively different behavior for D_q less than or greater than one:^{25,26,27}

$$\tilde{c}_q = \begin{cases} d(1 + D_q), & D_q \leq 1 \\ 2d\sqrt{D_q}, & D_q > 1 \end{cases} \quad (3.17)$$

Reversing the Galilean boost in Eq. (3.11) via Eq. (3.7), we see that

$$\begin{aligned} G_q(z, l \rightarrow \infty) &\sim h(z - c_q l), \\ c_q &\equiv \tilde{c}_q - \Xi q. \end{aligned} \quad (3.18)$$

Let us try to understand the physics implied by Eq. (3.18). The generating function $G_q(z, l)$ was defined via Eq. (3.6) in terms of the infinite tower of coupling constants $\{Y_{pq}\}$; the latter were introduced in the NL σ M definition of $F_q(\xi; L)$, Eq. (3.1). Under a change of length scale (e.g. an incremental increase in the sample size), each Y_{pq} evolves according to the RG Eq. (3.5). If we neglect the non-linear terms in this equation due to the OPE, then each non-zero Y_{pq} grows under renormalization according to its own scaling exponent $c_{pq}^{(0)} \equiv d - x_{pq}^*$; a full characterization of the system requires the specification of the entire set $\{c_{pq}^{(0)}\}$, $p \in \mathbb{N}$. As argued in Sec. I and below Eq. (3.5), we nevertheless expect that a single, well-defined exponent $\tau(q)$ can be defined for the IPR associated to a typical wavefunction, even in the limit of relatively “large” q . Eq. (3.18) implies that, through the OPE and the subsequent non-linearity of the KPP equation, the functional RG proves this assertion: the asymptotic scaling of $G_q(z, l)$ involves a single number, the velocity c_q given by Eqs. (3.17) and (3.18), which we can think of as a “typical” scaling exponent.

Since $G_q(z, l)$ tracks the scaling of coupling constants, we infer that the set $\{Y_{pq}\}$ “fuses” into a single, typical coupling Y_q^{typ} , up to less relevant perturbations to the critical NL σ M fixed point; we can then define an associ-

ated typical anomalous dimension

$$\begin{aligned} x_q^{\text{typ}} &\equiv d - c_q \\ &= \begin{cases} -\Xi q(q-1), & 1 \leq q \leq q_c \\ d(1-q) + q\left(\sqrt{d} - \text{sgn}(q)\sqrt{\Xi}\right)^2, & q > q_c \end{cases} \end{aligned} \quad (3.19)$$

where we have used Eq. (3.9). In this equation, the critical value q_c was defined in the Introduction, Eq. (1.10).

We infer from Eq. (3.19) that $F_q(\xi; L)$ acquires the following asymptotic form:

$$\begin{aligned} F_q(\xi; L \rightarrow \infty) &\sim \left\langle \exp\left[Y_q^{\text{typ}} \int d^d \mathbf{r} [\mathcal{O}_q^{\text{typ}}](\mathbf{r})\right] \right\rangle \\ &\sim \exp\left(Y_q^{\text{typ}} L^{d-x_q^{\text{typ}}}\right). \end{aligned} \quad (3.20)$$

As in Eq. (3.3), we have evaluated $F_q(\xi; L)$ in the lowest order cumulant expansion; the crucial difference between Eqs. (3.3) and Eq. (3.20) resides in the implied order of operations. To obtain the final result in Eq. (3.20), we first coarse grain the system, say by integrating-out short wavelength degrees of freedom (in a Wilsonian picture). The coarse graining generates higher order couplings $\{Y_{pq}\}$, $p > 1$, through the non-linear RG Eq. (3.5). In the large system size limit $l = \ln(L/L_0) \rightarrow \infty$, a single, well-defined typical coupling Y_q^{typ} emerges, associated to a new local operator $[\mathcal{O}_q^{\text{typ}}](\mathbf{r})$, whose scaling dimension is given by Eq. (3.19). Finally, we evaluate $F_q(\xi; L \rightarrow \infty)$ to lowest order in the cumulant expansion, which gives Eq. (3.20). This is expected to be a correct representation of the asymptotic scaling limit, because the functional RG has already built all of the most relevant operator “fusions” into the definition of $[\mathcal{O}_q^{\text{typ}}](\mathbf{r})$. The emergence of the associated Y_q^{typ} and x_q^{typ} has been proven above using the properties of the KPP equation, Eq. (3.8).

Finally, we extract the typical $\tau(q)$ spectrum. As obtained in the limit of large, but finite renormalization, the typical coupling Y_q^{typ} should have an analytic expansion in powers of the parameter ξ [c.f. Eqs. (3.2) and (3.15)]. Up to an irrelevant rescaling, we may write

$$Y_q^{\text{typ}} = -\xi - \sum_{m=2}^{\infty} \mathcal{Y}_{qm}^{\text{typ}} \xi^m. \quad (3.21)$$

Combining Eqs. (2.6) and (3.20), we obtain

$$\tau(q) \sim \frac{d}{d \ln L} \int_0^{\infty} \frac{d\xi}{\xi} \left[e^{Y_q^{\text{typ}} L^{d-x_q^{\text{typ}}}} - q e^{Y_1^{\text{typ}} L^{d-x_1^{\text{typ}}}} \right]. \quad (3.22)$$

In the limit $L \rightarrow \infty$, we may neglect all but the first term in Eq. (3.21), since $d - x_q^{\text{typ}} \geq 0$ for all $q \geq 1$, provided $\Xi \leq 4d$. This condition is always satisfied in the perturbatively accessible regime, $0 < \epsilon \ll 1$, where the parameter $\Xi = \sqrt{\epsilon/2} + \mathcal{O}(\epsilon) \ll 1$ [Eq. (1.6c)]. Then we obtain, using Eq. (2.5)

$$\tau(q) = d(q-1) + x_q^{\text{typ}} - q x_1^{\text{typ}}. \quad (3.23)$$

Eq. (3.23) for the typical $\tau(q)$ should be compared to Eq. (1.5) for $\tilde{\tau}(q)$. In the perturbative regime $\epsilon \ll 1$, we have $x_1^{\text{yp}} = 0$ [Eq. (3.19)]. Combining Eqs. (3.19) and (3.23), we arrive at our final result, the typical $\tau(q)$ spectrum given by

$$\tau(q) = \begin{cases} d(q-1) \left(1 - \frac{q}{q_c^2}\right), & |q| \leq q_c \\ d \left(1 - \frac{\text{sgn}(q)}{q_c}\right)^2 q, & |q| > q_c \end{cases} \quad (3.24)$$

where $q_c = \sqrt{d/\Xi}$ [Eq. (1.10)]. In this equation, we have extended q from the positive integers to the entire real line. The average $\tilde{\tau}(q)$ and typical $\tau(q)$ spectra are respectively sketched in the top and bottom panels of Fig. 1 in Sec. I.

The singularity spectrum $f(\alpha)$ was introduced in Eq. (1.2). The $f(\alpha)$ corresponding to the typical $\tau(q)$ in Eq. (3.24) is

$$f(\alpha) = \begin{cases} d - \frac{(\alpha - d - \Xi)^2}{4\Xi} \\ = \frac{q_c^2(\alpha_+ - \alpha)(\alpha - \alpha_-)}{4d}, & \alpha_- \leq \alpha \leq \alpha_+ \\ 0, & \alpha < \alpha_-, \alpha_+ < \alpha \end{cases} \quad (3.25)$$

The spectral cutoffs α_{\pm} were defined by Eq. (1.9). As expected, $f(\alpha)$ associated to the typical wavefunction is never negative, as discussed in Sec. I; see also the top and bottom panel insets in Fig. 1. Eqs. (3.24) and (3.25) hold to the lowest non-trivial order in $\sqrt{\epsilon}$. The consistency of the restriction to only the lowest order contributions in the ϵ expansion is demonstrated in Sec. IV.

An alternative representation of multifractality invokes the ‘‘generalized dimension’’ D_q , defined via

$$\tau(q) \equiv (q-1)D_q. \quad (3.26)$$

Spectral termination [Eqs. (3.24) and (3.25)] implies that $\alpha_+ \leq D_q \leq \alpha_-$, with the boundary values associated to the limits

$$\lim_{q \rightarrow \pm\infty} D_q = \alpha_{\mp}. \quad (3.27)$$

Numerical computations of D_q for the typical wavefunction confirm Eq. (3.27); see, e.g., Refs. 13 and 14.

C. Comparison with other arguments

Our final results (3.24) and (3.25) agree with previous heuristic arguments given in Refs. 37, 15, and 23. As explained below Eq. (1.2), $f(\alpha)$ describes the measure $L^{f(\alpha)}$ of the set of those points \mathbf{r} where the eigenfunction ψ takes the value $|\psi(\mathbf{r})|^2 \propto L^{-\alpha}$.¹⁰ Hence, the IPR P_q [Eq. (1.1)] can be estimated as an integral

$$P_q \sim \int_{f(\alpha) \geq 0} d\alpha L^{-q\alpha + f(\alpha)}. \quad (3.28)$$

The integrand takes a maximum value at a saddle point value α , which defines the $\tau(q)$. For $|q| < q_c$, this saddle point is in the integration domain, whereas for $|q| > q_c$ it is outside of it. In the latter case, the integral is dominated by the boundary value of $\alpha = \alpha_{\mp}$, where $f(\alpha_{\mp}) = 0$.

IV. DISCUSSION

We have provided a field theoretical description of the termination of the multifractal spectrum $\tau(q)$, as defined for the typical wavefunctions, at the Anderson MIT in $d = 2 + \epsilon$ for the unitary disordered metal class. The essential ingredients of the calculation are evident in the formulation of Eqs. (2.6) and (3.1): these are the infinite set of properly normalized LDOS moment operators $\{[\mathcal{O}_{pq}](\mathbf{r})\}$, $p \in \mathbb{N}$, characterized by the negative scaling dimensions $\{x_{pq}^*\}$ in Eqs. (1.6a)–(1.6c). Each successive higher moment operator with $p = \{1, 2, \dots\}$ constitutes a more strongly relevant perturbation to the critical RG fixed point that describes the MIT. Through the OPE [Eq. (1.11)], lower moments always generate higher ones, and a consistent treatment of the problem requires that the entire infinite hierarchy of LDOS moment operators is retained. Ordinarily, the advent of an infinity of relevant scaling directions should cast serious doubt upon the adequacy of single (or few) parameter scaling, at least with respect to the investigated critical point; remarkably, the FRG ‘‘absorbs’’ the entire LDOS moment tower, and through the (universal) properties of the long-time asymptotics of the KPP equation, renders in the end a single, *universal* prediction for the typical $\tau(q)$.

Physically, the relevant LDOS moments reflect the fact that a random critical point should be characterized by the distribution functions of physical quantities, rather than their mean, variance, or first few moments. The distribution of an observable in the presence of quenched disorder can become very broad, due to the influence of rare events.^{43,44,50,51,52} In principle, we need the functional renormalization group (FRG) to obtain scaling for the entire probability distribution.⁶⁴ For large q , the IPR, defined by Eq. (1.1) [or of its field theoretic generalization, Eq. (2.3)], constitutes such a broadly-distributed observable.^{2,12,15,22,23,28} By comparison, a universal $\tau(q)$ spectrum for the typical wavefunction obtains because the log of the IPR is self-averaging for all q .^{15,23}

Technically, the FRG method implemented in Sec. III is completely analogous to that employed previously^{25,26,27} in the study of certain special 2D disordered field theories, possessing an additional, ‘chiral’ symmetry.⁴⁸ [See the end of Sec. IB for a description of these chiral models.] As in this prior work, the FRG translates the infinite set of coupled flow equations (3.5) into the KPP Eq. (3.8) for a certain (auxiliary) generating function. Through the asymptotic solution of the KPP equation in the form of a propagating wavefront, the tower of relevant LDOS moment operators combines

via multiple OPEs into a single, typical operator (up to less relevant perturbations), characterized by the typical scaling dimension in Eq. (3.19). The final results for $\tau(q)$ and $f(\alpha)$ [Eqs. (3.24) and (3.25)] are obtained via the FRG for the unitary universality class, using only two inputs, evaluated at the MIT: **(i)** the scaling dimensions $\{x_q^*\}$ (associated to the *average* operator scaling, already known from previous work)^{8,32,33,34} and **(ii)** the OPE coefficient $C_{q,q'}^{q+q'}$, Eq. (3.4) (computed in Sec. V to lowest non-trivial order in $\sqrt{\epsilon}$). The former is specific to the unitary class, but we have shown that the latter takes exactly the same form in the chiral model calculations.^{25,26,27}

In treating the unitary class, we have chosen to work only to the lowest order in $t^* \propto \sqrt{\epsilon}$, i.e. to one loop. To this order, the resulting singularity spectrum $f(\alpha)$ given by Eq. (3.25) is purely quadratic over the region $\alpha_+ < \alpha < \alpha_-$ (the so-called “parabolic approximation”).^{4,5,17,18,19} We now discuss the consistency of working with the functional renormalization group to this order in the ϵ -expansion. Corrections to the LDOS moment scaling dimensions $\{x_q^*\}$ are already known to four loops,^{33,34}

$$x_q^* = -\sqrt{\frac{\epsilon}{2}}q(q-1) - \frac{3\zeta(3)}{8}\epsilon^2q^2(q-1)^2 + \mathcal{O}(\epsilon^{5/2}), \quad (4.1)$$

where $\zeta(z)$ denotes the Riemann zeta function. While the FRG method formally retains LDOS moment operators $\{\llbracket \mathcal{O}_q \rrbracket(\mathbf{r})\}$ to arbitrarily high orders in q , it is crucial to note that the termination of the typical $\tau(q)$ spectrum [Eq. (3.24)] occurs at the finite value $q = q_c$ [Eq. (1.10)]; to lowest order,

$$q_c^2 = 2\sqrt{2/\epsilon} + \mathcal{O}(1). \quad (4.2)$$

Evaluating the 4-loop scaling dimension in Eq. (4.1) at q_c , we obtain

$$x_{q=q_c}^* = -2 + (2\epsilon)^{1/4} + \mathcal{O}(\epsilon^{1/2}). \quad (4.3)$$

The one-loop approximation consists of retaining only the first term on the right-hand side (RHS) of Eq. (4.1), as well as the terms written explicitly on the RHS of each of Eqs. (4.2) and (4.3). At termination ($q = q_c$), the higher order loop corrections give rise to additional terms in Eq. (4.3) that are down by higher powers of $\epsilon^{1/4}$, and these can be consistently neglected for $\epsilon \ll 1$.

We cannot resist contemplating, at a very speculative level, a naive extrapolation of our one-loop results to moderate or even large ϵ . First, note that Eq. (3.19) implies the existence of a non-zero, typical scaling dimension x_1^{typ} for the first moment of the LDOS, when $q_c < 1$:

$$x_1^{\text{typ}} = d \left(1 - \frac{1}{q_c}\right)^2, \quad q_c < 1. \quad (4.4)$$

Using the lowest order result in Eq. (4.2), we then define

$$\begin{aligned} \epsilon_F &\equiv \epsilon(q_c = 1) \\ &\sim 8. \end{aligned} \quad (4.5)$$

At face value, a $x_1^{\text{typ}} > 0$ would imply that the typical LDOS *vanishes* at the MIT. Eq. (4.5) suggests that this becomes possible in the limit of large spatial dimensionality, $\epsilon > \epsilon_F$. Such a scenario does not contradict rigorous results^{45,46} which prove that the average, global DOS remains uncritical (constant) across the transition for any spatial dimension d . Indeed, Bethe lattice computations⁶ exhibit a typical LDOS that vanishes *exponentially* across the transition.⁶⁶ As the Bethe lattice can be equated with the limit of infinite spatial dimensionality,³ this picture in fact appears consistent with Eqs. (4.4) and (4.5) in the limit $\epsilon \rightarrow \infty$, where upon $x_1^{\text{typ}} \rightarrow \infty$.

It has been asserted³ that the upper critical dimension for Anderson localization occurs only at $d = \infty$, i.e., the Bethe lattice case. The naive extrapolation of the results of this paper to large ϵ suggests an alternate possibility. To motivate the basic underlying idea, we note that for $\epsilon > \epsilon_F$, the typical multifractal spectrum $\tau(q)$ defined by Eqs. (3.19) and (3.23) would take the form

$$\tau(q) = \begin{cases} -d \left(1 - \frac{q}{q_c}\right)^2, & |q| \leq q_c \\ \frac{2d}{q_c} (q - |q|), & |q| > q_c \end{cases} \quad (4.6)$$

This should be contrasted with Eq. (3.24), which assumed $q_c > 1$ [always the case in the perturbatively accessible regime, $0 < \epsilon \ll 1$ —see Eq. (4.2)]. Eq. (4.6) shows that $\tau(q) = 0$ for all $q \geq q_c$ when $q_c < 1$ ($\epsilon > \epsilon_F$). Thus the $\tau(q)$ spectrum “freezes” for dimensionalities above the threshold $d_F \equiv 2 + \epsilon_F$. An analogous freezing transition has been predicted^{22,25,26,27,37,38} for the 2D chiral Dirac models discussed at the end of Sec. IA; in these models, the transition occurs for quenched disorder fluctuation strengths larger than some threshold value. Unlike the unitary metal class discussed here, the chiral model freezing transition has been rigorously derived through strong randomness³⁸ and FRG arguments,^{25,26,27,36} which do not rely upon expansion in a small parameter. By comparison, Eqs. (4.4) and (4.6) lie well beyond the perturbatively accessible regime. Regardless, the freezing scenario suggests the intriguing possibility of a finite $d_F < \infty$ for Anderson localization in the normal metal classes, which could perhaps serve as a finite upper critical dimension.

V. OPERATOR PRODUCT EXPANSION AT THE ANDERSON FIXED POINT: PERTURBATIVE CALCULATION

In this final (technical) section, we provide a derivation of the LDOS moment operator algebra required for

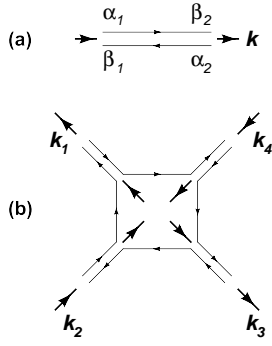


FIG. 2: Propagator (a) and lowest-order vertex (b) necessary for the one-loop RG, obtained by expanding Eq. (2.7) in terms of the unconstrained \hat{W} field, using Eq. (2.10). Associated amplitudes are given by Eqs. (5.1) and (5.2) in the text.

the functional RG construction in Sec. III. Using the NL σ M framework reviewed in Sec. II, we first rederive the anomalous scaling dimensions of the LDOS moment operators introduced in Sec. II C. We then turn to the perturbative evaluation of the operator product expansion, as defined by Eq. (1.11), between properly normalized versions of these eigenoperators.

A. Renormalization of the model

To begin, we consider the renormalization of the bare NL σ M defined by Eq. (2.7). This calculation is standard;^{1,42,67} we provide only our conventions necessary to set up the computation, and the corresponding results. Using the parameterization in Eq. (2.10), one obtains the $\hat{W} \rightarrow W^{\alpha}_{\beta}$ field propagator and vertex shown in Fig. 2. The propagator is pictured in Fig. 2(a) as pair of counter-directed thin lines, representing physically an ambulating electron-hole pair (‘diffuson’), and mathematically the linking of direct and conjugate indices in two inequivalent representations of $U(n)$ [since the maximum compact subgroup of $U(2n)$ is $U(n) \times U(n)$]. Equivalently, in the unitary class with this parameterization, the field W^{α}_{β} is Wick-contracted only with its adjoint $W^{\dagger\beta}_{\alpha}$; this fact is indicated by the thick arrows in Fig. 2, which also encode the direction of momentum flow. The amplitude corresponding to the propagator in Fig. 2(a) is

$$\langle W^{\alpha_1}_{\beta_1}(\mathbf{k}) W^{\dagger\alpha_2}_{\beta_2}(\mathbf{k}) \rangle = \delta_{\beta_2}^{\alpha_1} \delta_{\beta_1}^{\alpha_2} \frac{t_0}{|\mathbf{k}|^2 + h_0 t_0}, \quad (5.1)$$

where t_0 and h_0 are bare parameters. In this paper, we will only need the lowest order non-linear vertex $\equiv \mathfrak{V}_4$ [obtained via an expansion of Eq. (2.7) in powers of \hat{W}]; this vertex is pictured in Fig. 2(b), with the corresponding amplitude

$$\mathfrak{V}_4 = \frac{2!}{8t_0} \begin{bmatrix} 2(\mathbf{k}_1 \cdot \mathbf{k}_3 + \mathbf{k}_2 \cdot \mathbf{k}_4) - \mathbf{k}_1 \cdot \mathbf{k}_2 \\ -\mathbf{k}_2 \cdot \mathbf{k}_3 - \mathbf{k}_3 \cdot \mathbf{k}_4 - \mathbf{k}_4 \cdot \mathbf{k}_1 - 2h_0 t_0 \end{bmatrix}. \quad (5.2)$$

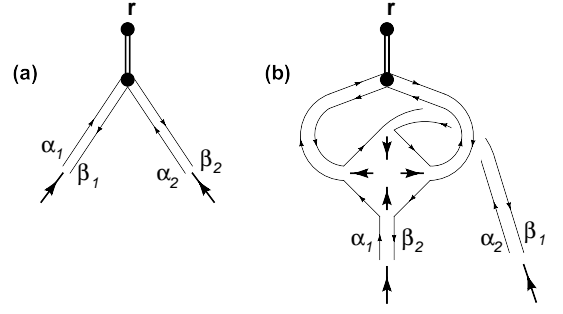


FIG. 3: Basic renormalization process of a composite operator.

Adopting standard dimensional regularization conventions,^{57,58,67}

$$\begin{aligned} t_0 &\equiv t\mu^{-\epsilon} F_t, \\ h_0 &\equiv Z_W^{-\frac{1}{2}} h, \end{aligned} \quad (5.3)$$

with t and h renormalized parameters, μ an arbitrary inverse-length scale, and Z_W the field renormalization of the elementary operator \hat{W} , the RG flow equations are given by

$$\begin{aligned} \frac{dt}{dl} &= \frac{-\epsilon t}{1 + \frac{d \ln F_t}{d \ln t}}, \\ \frac{d \ln h}{dl} &= d + \frac{1}{2} \frac{d \ln Z_W}{d \ln t} \frac{d \ln t}{dl}. \end{aligned} \quad (5.4)$$

In Eqs. (5.3) and (5.4), $d = 2 + \epsilon$ is the spatial dimensionality of the system, and $l \sim -\ln \mu$ is the logarithm of the spatial length scale.

For the compact unitary model with target space $U(2n)/U(n) \times U(n)$, the one-loop flow equations are

$$\frac{dt}{dl} = -\epsilon t + \frac{nt^2}{4\pi} + \mathcal{O}(t^3), \quad (5.5)$$

$$\frac{d \ln h}{dl} = d - \frac{nt}{4\pi} + \mathcal{O}(t^2). \quad (5.6)$$

These equations possess a critical fixed point at the ‘‘temperature’’ $t^* = 4\pi\epsilon/n$, with $h = 0$. The Anderson model corresponds to the limit $n \rightarrow 0$ in Eqs. (5.5) and (5.6); in this case, a non-trivial critical point occurs at two loop order.¹ In our conventions, the two-loop result is^{42,67}

$$\frac{dt}{dl} = -\epsilon t + \frac{t^3}{2^5 \pi^2} + \mathcal{O}(t^4), \quad (5.7)$$

valid in the limit $n \rightarrow 0$. The critical value of the inverse conductance at the metal-insulator transition in $d = 2 + \epsilon$ is proportional to $t^* = 4\pi\sqrt{2\epsilon} + \mathcal{O}(\epsilon)$.

B. Composite operator scaling dimensions

Next, we turn to the renormalization of the composite operators defined by Eq. (2.23). The renormalization of

$\mathcal{O}_{p[\beta_1\beta_2\dots\beta_p]}^{\alpha_1\alpha_2\dots\alpha_p}$ can be determined by considering “matrix elements” of that operator with arbitrary configurations of p distant, mutually separated adjoint fields $\{\hat{W}^\dagger{}_\gamma\}$. [For more general operators built out of products of both ‘ π ’ (\hat{W}, \hat{W}^\dagger) and ‘ σ ’ ($\sqrt{\hat{\mathbb{I}}_n - \hat{W}\hat{W}^\dagger}, \sqrt{\hat{\mathbb{I}}_n - \hat{W}^\dagger\hat{W}}$) components, one must typically consider multiple matrix element types involving different numbers of \hat{W} and \hat{W}^\dagger fields.⁵⁷]

Specifically, we define

$$\begin{aligned} \Gamma_p^{(0)}{}_{\gamma_1\dots\gamma_p}{}^{\lambda_1\dots\lambda_p}[\mathcal{O}_{p[\beta_1\dots\beta_p]}^{\alpha_1\dots\alpha_p}(\mathbf{r})] \\ \equiv \langle\langle \mathcal{O}_{p[\beta_1\dots\beta_p]}^{\alpha_1\dots\alpha_p}(\mathbf{r}) W^{\dagger\lambda_1}_{\gamma_1} \dots W^{\dagger\lambda_p}_{\gamma_p} \rangle\rangle, \end{aligned} \quad (5.8)$$

where the double angle brackets $\langle\langle \mathcal{O} \dots \rangle\rangle$ signify the one-particle irreducible matrix element of \mathcal{O} , amputating the external fields.^{58,68} The external $\{\hat{W}^\dagger\}$ fields are assumed to be located far from each other, and from the position \mathbf{r} of the composite operator. The superscript (0) on the left-hand side (LHS) of this equation indicates that this is a bare (i.e. not yet renormalized) quantity.

The basic one-loop process is illustrated in Fig. 3. Fig. 3(a) depicts the two-field matrix element of the (un-symmetrized) operator

$$W^{\alpha_1}{}_{\beta_1} W^{\alpha_2}{}_{\beta_2}(\mathbf{r}). \quad (5.9)$$

The vertex \mathfrak{V}_4 [Fig. 2(b) and Eq. (5.2)] pairwise permutes the lower indices of composite operator “legs,” as shown in Fig. 3(b). The completely antisymmetrized operator defined by Eq. (2.23) is clearly an eigenoperator at one loop, since the sum of all diagrams to this order represents a complete symmetrization procedure. This is expected to hold to all higher orders in t , because $\mathcal{O}_{p[\beta_1\dots\beta_p]}^{\alpha_1\dots\alpha_p}$ plays the role of a “highest weight state” in an irreducible representation of the full NL σ M target manifold symmetry group $U(2n)$.

At one loop, the matrix element defined by Eq. (5.8) is equal to

$$\begin{aligned} \Gamma_p^{(0)}{}_{\gamma_1\dots\gamma_p}{}^{\lambda_1\dots\lambda_p}[\mathcal{O}_{p[\beta_1\dots\beta_p]}^{\alpha_1\dots\alpha_p}(\mathbf{r})] \\ \sim \left[1 - \frac{p(p-1)}{2} I_1\right] \mathfrak{A}_{p[\beta_1\dots\beta_p]}^{\lambda_1\dots\lambda_p; \alpha_1\dots\alpha_p}, \end{aligned} \quad (5.10)$$

where $\mathfrak{A}_{p[\beta_1\dots\beta_p]}^{\lambda_1\dots\lambda_p; \alpha_1\dots\alpha_p}$ is the zeroth order amplitude [equal to zero or the pure constant $(1/p!)^2$, depending upon the matrix element].⁶⁹ In order to save writing wherever possible, from this place forward we will adopt the following shorthand notation: underlined vertices ($\underline{\Gamma}$), operators ($\underline{\mathcal{O}}$), and tree level matrix elements ($\underline{\mathfrak{A}}$) should be understood as possessing the appropriate set of indices, and all indices in a given equation are matched (in the appropriate order). With these conventions established, Eq. (5.10) may be rewritten compactly as

$$\underline{\Gamma}_p^{(0)}[\underline{\mathcal{O}}_p(\mathbf{r})] \sim \left[1 - \frac{p(p-1)}{2} I_1\right] \underline{\mathfrak{A}}_p. \quad (5.11)$$

In Eqs. (5.10) and (5.11),

$$\begin{aligned} I_1 &= \frac{-t_0}{2} \int \frac{d^d \mathbf{k}}{(2\pi)^d} \frac{1}{|\mathbf{k}|^2 + h_0 t_0} \\ &\sim \frac{t}{4\pi} \left[\frac{1}{\epsilon} + \frac{1}{2} \ln \left(\frac{h t e^\gamma}{4\pi \mu^2} \right) \right]. \end{aligned} \quad (5.12)$$

Here, we have used Eq. (5.3) and standard dimensional regularization technology; γ denotes the Euler-Mascheroni constant.

To renormalize Eq. (5.11), we insist that⁵⁸

$$Z_p^{-1} Z_W^{p/2} \underline{\Gamma}_p^{(0)}[\underline{\mathcal{O}}_p(\mathbf{r})] = \text{finite}, \quad (5.13)$$

where Z_p is the composite operator renormalization, and the factor of $Z_W^{p/2}$ compensates for the p (amputated) external fields. One then obtains the scaling dimension

$$\begin{aligned} x_p &= \epsilon \frac{d \ln Z_p}{d \ln t} \\ &= \frac{t}{4\pi} \left[np - \frac{p(p-1)}{2} \right] + \mathcal{O}(t^2). \end{aligned} \quad (5.14)$$

We make two observations. First, by evaluating Eq. (5.14) at the Anderson transition critical point located by $t^* = 4\pi\sqrt{2\epsilon}$, with $n \rightarrow 0$, we recover the known results^{32,34} for the multifractal spectrum $\tilde{\tau}(p)$ associated to the *averaged* IPR, as provided above in Eqs. (1.5)–(1.6c). Second, we have only considered the renormalization of the fully antisymmetrized operator defined by Eq. (2.23), because this is the most relevant in the $n \rightarrow 0$ limit. The fully *symmetrized* operator $\mathcal{O}_{p(\beta_1\beta_2\dots\beta_p)}^{\alpha_1\alpha_2\dots\alpha_p}$, which is defined as in Eq. (2.23) without the $\text{sgn}(\mathbf{P})$ factor in the summand, also constitutes an eigenoperator with scaling dimension

$$x_{p(\text{sym})} = \frac{t}{4\pi} \left[np + \frac{p(p-1)}{2} \right] + \mathcal{O}(t^2). \quad (5.15)$$

Consider the case of $n = 1$. The fully antisymmetrized operator defined by Eq. (2.23) does not exist for $p > 1$, since all $\hat{W} \Rightarrow W$ fields are scalars in this case. At the fixed point located by $t^* = 4\pi\epsilon/n$ with $n = 1$, the symmetrized operator scaling dimension $x_{p(\text{sym})}^* = \epsilon p(p+1)/2 + \mathcal{O}(\epsilon^2)$, which is the expected result for spherical harmonic composite operators in the $U(2)/U(1) \times U(1) \sim O(3)/O(2)$ NL σ M.⁵⁷

C. Two-point function normalization at the MIT

The set of coefficients $\{C_{q,q'}^{g+g'}\}$ [Eq. (1.11)] defining the operator product expansion (OPE) for *properly normalized* composite eigenoperators constitute universal numbers characterizing the MIT. The proper (RG scheme-dependent) normalization of each eigenoperator is such that its two-point autocorrelation function is scheme-independent at the critical point in $d = 2 + \epsilon$.⁶² In this

subsection, we derive the normalization of the operators defined by Eq. (2.23) with respect to their two-point functions (at large spatial separation), while the OPE is considered in the sequel. Since we are interested in critical properties, we assume $h = 0$ in Eq. (2.7) throughout the following discussion.

The technical tool for computing operator correlation functions at any perturbatively accessible fixed point is RG-improved perturbation theory (PT). In the case of the non-trivial NL σ M critical point in $d = 2 + \epsilon$, however, some technical difficulties arise: For a NL σ M with a compact, non-Abelian symmetry, the trivial fixed point located at $t = 0$ is invariably infrared (IR) unstable in 2D.⁵⁸ For any nonzero t , such a 2D model always flows under the RG toward a symmetry-restored, thermally-disordered “paramagnetic” state. Renormalized perturbation theory at $t \ll 1$, for composite operator correlators that are *not* invariant under the full symmetry group of the sigma model target manifold, is typically plagued by IR divergences, and hence affected by the specific way one regularizes these IR divergences.

The solution^{70,71,72} that we employ in this section is to consider only invariant correlation functions. Invariant correlators are free of IR divergences, and a sensible renormalized PT for these objects can be constructed.⁷³ For the OPE in the next section, we will see that this restriction is unnecessary.

We stress that, by the same token, *all* eigenoperators at the non-trivial fixed point in $d = 2 + \epsilon$ possess well-defined critical correlations. Thus the above-described calculational impasse, as well as its solution, in fact reflect peculiarities of the ϵ -expansion, rather than the NL σ M itself (at least for $d > 2$).

Within the symmetry-broken phase, ‘ π ’ (\hat{W}, \hat{W}^\dagger) and ‘ σ ’ ($\sqrt{\hat{\mathbb{I}}_n - \hat{W}\hat{W}^\dagger}, \sqrt{\hat{\mathbb{I}}_n - \hat{W}^\dagger\hat{W}}$) fields possess very different correlation functions: the former constitute Gold-

stone modes with massless correlations, while the latter are gapped longitudinal modes, with massive correlation functions for all $t < t^*$. At the critical point $t = t^*$ for $n > 0$, symmetry is restored; here, all operators belonging to a given irreducible representation of the target manifold symmetry group will possess identical correlations, provided a group-invariant normalization is chosen for these operators. [For the O(3)/O(2) model, an invariant normalization is that conventionally assigned to spherical harmonics, written in terms of π and σ coordinates.] We will use this fact to determine the two-point function normalization of $\mathcal{O}_p^{\alpha_1 \alpha_2 \dots \alpha_p}_{[\beta_1 \beta_2 \dots \beta_p]}$ [Eq. (2.23)] for $n = \{1, 2, \dots\}$, and then continue the result to $n \rightarrow 0$.

Consider the following invariant, “non-local” operator,

$$\Omega_p(\mathbf{r}, \mathbf{r}') \equiv \sum_{\{m\}} \Theta_{p\{m\}}(\mathbf{r}) \Theta_{p\{m\}}^*(\mathbf{r}'), \quad (5.16)$$

where $\Theta_{p\{m\}}$ is a composite operator that is a component of an irreducible representation of the sigma model symmetry group. The representation is distinguished by the Casimir parameter p , while the component operators are labeled by a set of “magnetic” quantum numbers $\{m\}$, e.g. $\{\alpha_1, \dots, \alpha_p, [\beta_1, \dots, \beta_p]\} \in \{m\}$ for the antisymmetrized LDOS moment operators defined by Eq. (2.23). One may use expressions for the $\Theta_{p\{m\}}$ in terms of the target manifold coordinates ($\hat{W}, \hat{W}^\dagger, \sqrt{\hat{\mathbb{I}}_n - \hat{W}\hat{W}^\dagger}, \sqrt{\hat{\mathbb{I}}_n - \hat{W}^\dagger\hat{W}}$) in order to construct an explicit expression for the RHS of Eq. (5.16); at the non-trivial critical point in $d = 2 + \epsilon$, however, we require only the lowest order expansion for the *expectation* of Eq. (5.16) in powers of $t^* \propto \epsilon^\sigma$ ($\sigma = 1$ or $1/2$ for $n \in \mathbb{N}$ or $n \rightarrow 0$, respectively). Since an expansion in powers of t is equivalent to an expansion in powers of \hat{W} and \hat{W}^\dagger , we make the following ansatz:

$$\Omega_p(\mathbf{r}, \mathbf{r}') \sim \tilde{\alpha}_p \left(1 + \frac{\alpha_{p,1}}{2n^2} \text{Tr} \left[\hat{W}^\dagger(\mathbf{r}) \hat{W}(\mathbf{r}') - \hat{W}^\dagger(\mathbf{r}) \hat{W}(\mathbf{r}) + \hat{W}^\dagger(\mathbf{r}') \hat{W}(\mathbf{r}) - \hat{W}^\dagger(\mathbf{r}') \hat{W}(\mathbf{r}') \right] + \mathcal{O}(\hat{W}^4) \right). \quad (5.17)$$

The expectation of the assumed form of Eq. (5.17) is free from IR divergences. While the numerical coefficient $\tilde{\alpha}_p$ in this equation is arbitrary, $\alpha_{p,1}$ is not, and can in principle be computed from knowledge of the representation theory of the NL σ M symmetry group; instead, we will determine its value empirically, below. Note that Eq. (5.17) is manifestly invariant under $U(n) \times U(n)$ subgroup transformations, $\hat{W} \rightarrow \hat{U}_L \hat{W} \hat{U}_R$, with $\hat{U}_{L/R}^\dagger \hat{U}_{L/R} = \hat{\mathbb{I}}_n$.

We compute the expectation of Eq. (5.17) in position space,⁷¹ using the IR-convergent Green’s function at zero

coupling

$$\begin{aligned} & \langle W^{\dagger \alpha_1}_{\beta_1}(\mathbf{r}) W^{\alpha_2}_{\beta_2}(0) - W^{\dagger \alpha_1}_{\beta_1}(0) W^{\alpha_2}_{\beta_2}(0) \rangle_0 \\ &= \delta_{\beta_2}^{\alpha_1} \delta_{\beta_1}^{\alpha_2} t_0 \int \frac{d^d \mathbf{k}}{(2\pi)^d} \frac{e^{i\mathbf{k} \cdot \mathbf{r}} - 1}{|\mathbf{k}|^2} \\ &= \delta_{\beta_2}^{\alpha_1} \delta_{\beta_1}^{\alpha_2} \frac{t_0}{(d-2)S_d} \frac{1}{|\mathbf{r}|^{d-2}} \\ &\sim \delta_{\beta_2}^{\alpha_1} \delta_{\beta_1}^{\alpha_2} \frac{t}{2\pi} \left[\frac{1}{\epsilon} - \frac{1}{2} \ln(\pi \mu^2 |\mathbf{r}|^2 e^\gamma) \right], \quad (5.18) \end{aligned}$$

where S_d is the surface area of the sphere in d dimensions, and we have used Eqs. (5.1) and (5.3).

Let us define the renormalized operator

$$[\Omega_p](\mathbf{r}, \mathbf{r}') \equiv Z_p^{-2} \Omega_p(\mathbf{r}, \mathbf{r}'), \quad (5.19)$$

where Z_p is the renormalization factor obtained via Eqs. (5.13) and (5.14) for the composite operators defined by Eq. (2.23); all operators belonging to a particular irreducible representation receive the same renormalization in a NL σ M.⁵⁷

Insisting that $\langle [\Omega_p](\mathbf{r}, \mathbf{r}') \rangle$ is finite (for $\mathbf{r} \neq \mathbf{r}'$), we see that we must take

$$\alpha_{p,1} = np - \frac{p(p-1)}{2} \quad (5.20)$$

in Eq. (5.17). We have obtained the lowest order expansion coefficient for the group-invariant structure defined by Eqs. (5.16) and (5.17) without explicitly employing group theory, but using only the renormalizability of the NL σ M! [Basic group theoretic knowledge was necessary to identify the invariant scaling operators defined by Eq. (2.23), however.]⁷⁴

Finally, we set $t = t^*(\epsilon)$, and then we re-exponentiate the expectation of Eq. (5.19) to obtain, at the non-trivial critical point,

$$\langle [\Omega_p](\mathbf{r}, \mathbf{r}') \rangle \sim \frac{\tilde{\alpha}_p (\pi\mu^2 e^\gamma)^{-x_p^*}}{|\mathbf{r} - \mathbf{r}'|^{2x_p^*}}, \quad (5.21)$$

where x_p^* is the scaling dimension in Eq. (5.14), evaluated at $t = t^*$. [x_p^* is given explicitly by Eqs. (1.6a)–(1.6c) for the limit $n \rightarrow 0$, appropriate to the MIT.]

Eq. (5.21) allows us to define the following “renormalized and normalized” composite operators, which we will enclose with the double square brackets $[\![\cdot \cdot]\!]$. Referring to Eq. (2.23), we designate

$$[\![\mathcal{O}_{p[\beta_1 \dots \beta_p]}^{\alpha_1 \dots \alpha_p}]\!] (\mathbf{r}) \equiv Z_p^{-1} (\pi\mu^2 e^\gamma)^{\frac{x_p^*}{2}} \mathcal{O}_{p[\beta_1 \dots \beta_p]}^{\alpha_1 \dots \alpha_p} (\mathbf{r}). \quad (5.22)$$

Eqs. (5.19) and (5.21) guarantee that the two-point correlation function between distant operators defined by Eq. (5.22) is both ultraviolet finite, and independent of the renormalization scheme.

D. Operator product expansion at the MIT

We conclude this section with the construction of the operator product expansion (OPE) for the operators in Eq. (5.22). At the critical point in $d = 2 + \epsilon$, the OPE is expected to take the form

$$\begin{aligned} & [\![\mathcal{O}_{p[\beta_1 \dots \beta_p]}^{\alpha_1 \dots \alpha_p}]\!] (\mathbf{r}) [\![\mathcal{O}_{p'[\beta'_1 \dots \beta'_{p'}]}^{\alpha'_1 \dots \alpha'_{p'}}]\!] (\mathbf{r}') \\ & \sim \frac{C_{p,p'}^{p+p'}}{|\mathbf{y}|^{x_p^* + x_{p'}^* - x_{p+p'}^*}} [\![\mathcal{O}_{p+p'[\beta_1 \dots \beta_p \beta'_1 \dots \beta'_{p'}]}^{\alpha_1 \dots \alpha_p \alpha'_1 \dots \alpha'_{p'}}]\!] (\mathbf{R}) + \dots, \end{aligned} \quad (5.23)$$

where $\mathbf{y} \equiv \mathbf{r} - \mathbf{r}'$, $\mathbf{R} \equiv (\mathbf{r} + \mathbf{r}')/2$, x_p^* is the scaling dimension defined by Eqs. (5.14) and (1.6a)–(1.6c), and $C_{p,p'}^{p+p'}$ is the (universal) OPE coefficient that we seek, expected to possess an expansion in powers of $t^*(\epsilon)$. Eq. (5.23) will hold as a replacement rule in the limit $|\mathbf{y}| \rightarrow 0$, valid inside correlation functions involving arbitrary configurations of other, spatially remote operators. Note that Eq. (5.23) relates a product of maximally antisymmetric operators to a single, maximally antisymmetric operator; the ellipsis “...” on the right-hand side (RHS) of this equation represents other, less relevant operators that are produced in the ‘fusion’ process; we will ignore the contribution of the latter to functional RG.⁷⁵

In order to determine $C_{p,p'}^{p+p'}$, we compute an arbitrary matrix element $\Gamma_{p+p' \gamma_1 \dots \gamma_{p+p'}}^{\lambda_1 \dots \lambda_{p+p'}} [\dots]$ of both sides of Eq. (5.23), as defined by Eq. (5.8). Using Eqs. (5.10) and (5.22), and employing the compact notation introduced above and implemented in Eq. (5.11), the RHS of Eq. (5.23) may be written as

$$\begin{aligned} \underline{\Gamma}_{p+p'}[\underline{\text{RHS}}] &= Z_W^{\frac{p+p'}{2}} Z_{p+p'}^{-1} (\pi\mu^2 e^\gamma)^{\frac{x_{p+p'}^*}{2}} \frac{C_{p,p'}^{p+p'}}{|\mathbf{y}|^{x_p^* + x_{p'}^* - x_{p+p'}^*}} \\ &\times \underline{\Gamma}_{p+p'}^{(0)}[\underline{\mathcal{O}}_{p+p'}(\mathbf{R})], \end{aligned} \quad (5.24)$$

where Z_W ($Z_{p+p'}$) is the field strength (composite operator) renormalization factor, and the bare amplitude is given by

$$\underline{\Gamma}_{p+p'}^{(0)}[\underline{\mathcal{O}}_{p+p'}] = \left[1 - \frac{1}{2}(p+p')(p+p'-1)I_1 \right] \underline{\mathfrak{A}}_{p+p'}. \quad (5.25)$$

In Eq. (5.25), I_1 is the loop integral defined by Eq. (5.12), where we retain the infrared regularization for now, $h_0 \neq 0$, while

$$\underline{\mathfrak{A}}_{p+p'} \rightarrow \underline{\mathfrak{A}}_{p+p' \gamma_1 \dots \gamma_{p+p'}; [\beta_1 \dots \beta_p \beta'_1 \dots \beta'_{p'}]}^{\lambda_1 \dots \lambda_{p+p'}; \alpha_1 \dots \alpha_p \alpha'_1 \dots \alpha'_{p'}}$$

denotes the zeroth order amplitude for the matrix element (a pure number). (See footnote 69 for details.)

Similarly, the LHS matrix element of Eq. (5.23) may be written

$$\begin{aligned} \underline{\Gamma}_{p+p'}[\underline{\text{LHS}}] &= Z_W^{\frac{p+p'}{2}} Z_p^{-1} Z_{p'}^{-1} (\pi\mu^2 e^\gamma)^{\frac{x_p^* + x_{p'}^*}{2}} \\ &\times \underline{\Gamma}_{p+p'}^{(0)}[\underline{\mathcal{O}}_p(\mathbf{r}) \underline{\mathcal{O}}_{p'}(\mathbf{r}')], \end{aligned} \quad (5.26)$$

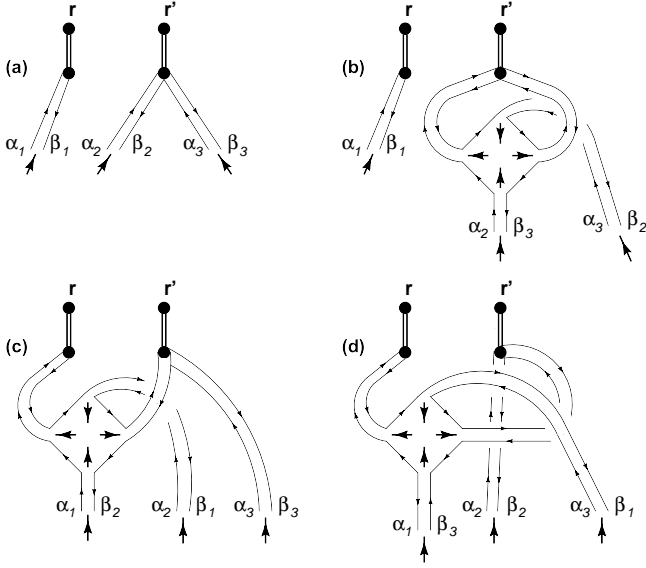


FIG. 4: Basic renormalization process in the OPE.

where the bare (unrenormalized) amplitude is

$$\begin{aligned} & \underline{\Gamma}_{p+p'}^{(0)}[\underline{\mathcal{O}}_p(\mathbf{r})\underline{\mathcal{O}}_{p'}(\mathbf{r}')] \\ & \rightarrow \langle\langle \underline{\mathcal{O}}_p^{\alpha_1 \dots \alpha_p}_{[\beta_1 \dots \beta_p]}(\mathbf{r}) \underline{\mathcal{O}}_{p'}^{\alpha'_1 \dots \alpha'_{p'}}_{[\beta'_1 \dots \beta'_{p'}]}(\mathbf{r}') \\ & \quad \times W^{\dagger \lambda_1}_{\gamma_1} \dots W^{\dagger \lambda_{p+p'}}_{\gamma_{p+p'}} \rangle\rangle \end{aligned} \quad (5.27a)$$

$$\begin{aligned} & = \frac{1}{(p!p')^2} \langle\langle W^{\alpha_1 \beta_1} \dots W^{\alpha_p \beta_p}(\mathbf{r}) \\ & \quad \times W^{\alpha'_1 \beta'_1} \dots W^{\alpha'_{p'} \beta'_{p'}}(\mathbf{r}') \\ & \quad \times W^{\dagger \lambda_1}_{\gamma_1} \dots W^{\dagger \lambda_{p+p'}}_{\gamma_{p+p'}} \rangle\rangle \\ & + \left\{ \begin{array}{l} (p!p' - 1) \text{ other terms} \\ \text{obtained by permutations} \end{array} \right\}. \end{aligned} \quad (5.27b)$$

As in Eq. (5.8), the external fields $\{\hat{W}^\dagger\}$ in these equations are assumed to be located far from the vicinity of the operator product (\mathbf{r} or \mathbf{r}') and from each other, while the double angle brackets instruct us to take the one-particle irreducible amplitude, with external legs amputated.⁵⁸

Consider the one-loop renormalization of the term written explicitly in Eq. (5.27b); the other $(p!p' - 1)$ terms implied in this equation will give identical contributions. The basic renormalization process of an operator product is illustrated in Fig. 4 specifically for the combination

$$W^{\alpha_1 \beta_1}(\mathbf{r}) \otimes W^{\alpha_2 \beta_2}(\mathbf{r}') W^{\alpha_3 \beta_3}(\mathbf{r}').$$

The vertex \mathfrak{V}_4 [Fig. 2 and Eq. (5.2)] modifies the operator product in two ways. First, it renormalizes the constituent operators, pairwise permuting indices of legs both tied to either \mathbf{r} or \mathbf{r}' , as shown in Fig. 4(b) [c.f.

Fig. 3]. Second, \mathfrak{V}_4 ties the two operators together by pairwise crosspermuting their indices, as depicted in Figs. 4(c) and (d).

Now, algebraically we may express an unsymmetrized product of q \hat{W} -field matrix elements ($W^{\alpha\beta}$) in terms of the completely antisymmetrized product, native to the most relevant irreducible representation with Casimir parameter q of the $\text{NL}\sigma\text{M}$ symmetry group, plus other terms which belong to other (completely symmetric or mixed symmetry) representations. In particular,

$$W^{\alpha_1 \beta_1} \dots W^{\alpha_q \beta_q} = W^{\alpha_1 [\beta_1 \dots W^{\alpha_q \beta_q]} + \dots, \quad (5.28)$$

where again the square brackets $[\dots]$ denote complete antisymmetrization. The unity coefficient in front of the completely antisymmetrized tensor on the RHS of Eq. (5.28) follows from the fact that the antisymmetrization procedure is a projective operation that kills symmetric or mixed symmetry terms, but leaves the pre-antisymmetrized component invariant.

After the vertex acts upon the unsymmetrized operator product displayed explicitly in Eq. (5.27b), giving the appropriate factors for the two types of renormalization depicted in Fig. 4(b) and Figs. 4(c),(d), respectively, we are free to use Eq. (5.28) to replace each resulting unsymmetrized, permuted product with the corresponding completely antisymmetrized version, up to less relevant mixed symmetry or higher gradient terms.⁷⁶ The completely antisymmetrized product of $p + p'$ factors is just the composite operator on the RHS of the OPE, as defined by Eq. (5.23). Therefore, using the Feynman rules in Eqs. (5.1) and (5.2), and summing all diagram topologies to one loop, Eq. (5.27a) may be written as

$$\begin{aligned} & \underline{\Gamma}_{p+p'}^{(0)}[\underline{\mathcal{O}}_p(\mathbf{r})\underline{\mathcal{O}}_{p'}(\mathbf{r}')] \\ & \sim \binom{p+p'}{p} \left(\begin{array}{l} 1 - I_1 \left[\frac{p(p-1)}{2} + \frac{p'(p'-1)}{2} \right] \\ - I_2(\mathbf{y}) [pp'] \end{array} \right) \underline{\mathfrak{A}}_{p+p'}, \end{aligned} \quad (5.29)$$

where $\underline{\mathfrak{A}}_{p+p'}$ denotes the zeroth order matrix element of $\underline{\mathcal{O}}_{p+p'}^{\alpha_1 \dots \alpha_p \alpha'_1 \dots \alpha'_{p'}}_{[\beta_1 \dots \beta_p \beta'_1 \dots \beta'_{p'}]}$, as in Eq. (5.25), I_1 is the integral defined by Eq. (5.12), and

$$I_2(\mathbf{y}) = \frac{-t_0}{2} \int \frac{d^d \mathbf{k}}{(2\pi)^d} \frac{e^{i\mathbf{k}\cdot\mathbf{y}}}{|\mathbf{k}|^2 + h_0 t_0}. \quad (5.30)$$

Let us briefly comment upon the origin of the various combinatoric factors in Eq. (5.29): The prefactor $\binom{p+p'}{p}$ originates from the normalization convention used in Eq. (2.23). The factors of $p(p-1)/2$ and $p'(p'-1)/2$ count the number of inequivalent ways leg indices associated with *either* operator $\underline{\mathcal{O}}_p$ or $\underline{\mathcal{O}}_{p'}$ (but not both) may be permuted, as occurred previously in the scaling dimension calculation [Eq. (5.10)]. The factor of pp' counts the number of inequivalent ways one leg index from each operator may be interpermutated, as in Figs. 4(c),(d).

Equating the left-hand and right-hand sides of the OPE, Eqs. (5.24)–(5.26) and (5.29), and expanding everything to the lowest non-trivial order in t , we obtain

$$C_{p,p'}^{p+p'} \sim \binom{p+p'}{p} \begin{pmatrix} 1 + pp' [I_1 - I_2(\mathbf{y})] + \ln \left[\frac{Z_{p+p'}}{Z_p Z_{p'}} \right] \\ -\frac{1}{2}(x_{p+p'}^* - x_p^* - x_{p'}^*) \\ \times \ln(\pi\mu^2 |\mathbf{y}|^2 e^\gamma) \end{pmatrix}. \quad (5.31)$$

We may now take the limit $h_0 \rightarrow 0$, because the combination $2[I_1 - I_2(\mathbf{y})]$ [Eqs. (5.12) and (5.30)] gives the IR-finite integral evaluated previously in Eq. (5.18), above. Using Eq. (5.14), Eq. (5.31) simplifies to the expression

$$C_{p,p'}^{p+p'} \sim \binom{p+p'}{p} \begin{pmatrix} 1 - \frac{1}{2} \left(x_{p+p'}^* - x_p^* - x_{p'}^* + t \frac{pp'}{4\pi} \right) \\ \times \ln(\pi\mu^2 |\mathbf{y}|^2 e^\gamma) \end{pmatrix}. \quad (5.32)$$

In general, the RHS of this equation is a UV-finite, non-zero function of the operator separation \mathbf{y} . At the non-trivial critical point $t = t^*$ in $d = 2 + \epsilon$, however, we have [from Eq. (5.14)]

$$C_{p,p'}^{p+p'} \sim \binom{p+p'}{p} + \mathcal{O}(t^{*2}). \quad (5.33)$$

At the Anderson metal-insulator transition ($n \rightarrow 0$), $t^* = 4\pi\sqrt{2}\epsilon + \mathcal{O}(\epsilon)$. Thus the OPE coefficient for the operators with normalization determined by Eq. (5.22) is *independent* of $\sqrt{\epsilon}$ to order ϵ .⁷⁸

The result in Eq. (5.33) should be contrasted with a similar computation in ϕ^4 theory in $d = 4 - \epsilon$: at the Wilson-Fisher fixed point, the fusion of two elementary renormalized and normalized $[\phi]$ fields into the mass operator $[\phi^2]$ yields an OPE coefficient that acquires a correction at the lowest non-trivial order in the quartic coupling strength $\lambda^* \propto \epsilon + \mathcal{O}(\epsilon^2)$. (See, e.g., Ref. 79.) As in the above NL σ M calculation, the normalization of the operators $[\phi]$ and $[\phi^2]$ is chosen so as to give two-point autocorrelation functions independent of the renormalization scheme.

Finally, tracing over pairs of indices in Eq. (5.23) allows the OPE to be written as

$$[\mathcal{O}_p](\mathbf{r}) [\mathcal{O}_{p'}](\mathbf{r}') \sim \frac{C_{p,p'}^{p+p'}}{|\mathbf{y}|^{x_p^* + x_{p'}^* - x_{p+p'}^*}} [\mathcal{O}_{p+p'}](\mathbf{R}) + \dots, \quad (5.34)$$

where

$$\begin{aligned} [\mathcal{O}_p](\mathbf{r}) &\equiv \sum_{\alpha_1=1}^n \dots \sum_{\alpha_p=1}^n [\mathcal{O}_p^{\alpha_1 \dots \alpha_p}](\mathbf{r}) \\ &= Z_p^{-1} (\pi\mu^2 e^\gamma)^{\frac{x_p^*}{2}} \mathcal{O}_p(\mathbf{r}) \end{aligned} \quad (5.35)$$

is the renormalized and normalized version of the bare operator defined by Eq. (2.24).

The OPE in Eq. (5.34), together with the coefficient $C_{p,p'}^{p+p'}$ given by Eq. (5.33), constitutes the primary technical result of this paper. We have succeeded in associating a unique, properly normalized operator $[\mathcal{O}_p](\mathbf{r})$ to the p^{th} moment of the LDOS, and demonstrated that the family of such operators obeys the OPE set forth in Eq. (1.11) in the Introduction. This is the necessary input to the functional RG scheme used in Sec. III to extract the typical multifractal spectrum $\tau(q)$ in Eq. (3.24).

Acknowledgments

We would like to thank Igor Aleiner, Boris Altshuler, and Gabriel Kotliar for helpful discussions and probing questions. This work was supported in part by the Nanoscale Science and Engineering Initiative of the National Science Foundation under NSF Award Number CHE-06-41523, and by the New York State Office of Science, Technology, and Academic Research (NYS-TAR) (M.S.F.). This work was also supported in part by the NSF under Grants No. DMR-0547769 (M.S.F.), PHY05-51164 (S.R.), and DMR-0706140 (A.W.W.L.). S.R. thanks the Center for Condensed Matter Theory at University of California, Berkeley for its support.

* Electronic address: psiborf@rci.rutgers.edu

¹ For a review, see, e.g., P. A. Lee and T. V. Ramakrishnan, Rev. Mod. Phys. **57**, 287 (1985); B. L. Altshuler and B. D. Simons in *Proceedings of the Les Houches Summer School on Mesoscopic Quantum Physics*, edited by E. Akkermans, G. Montambaux, J. L. Pichard, and J. Zinn-Justin (Elsevier, Amsterdam, 1995).

² A. D. Mirlin, Phys. Rep. **326**, 259 (2000); in “New Directions in Quantum Chaos” (Proceedings of the International School of Physics “Enrico Fermi,” Course CXLIII), Eds. G. Casati, I. Guarneri, and U. Smilansky (IOS Press, Amsterdam, 2000), pp. 223-298.

³ For a recent review, see, e.g., F. Evers and A. D. Mirlin, Rev. Mod. Phys. **80**, 1355 (2008).

⁴ For a review, see M. Janssen, Int. J. Mod. Phys. B **8**, 943 (1994).

⁵ For a review, see B. Huckestein, Rev. Mod. Phys. **67**, 357 (1995).

⁶ K. Efetov, *Supersymmetry in disorder and chaos* (Cambridge University Press, Cambridge, 1997).

⁷ The notion of the multifractality was recently extended to the wavefunction statistics at surfaces (boundaries) (‘surface multifractality’) of a bulk disordered electronic system at criticality: A. R. Subramaniam, I. A. Gruzberg, A. W.

- W. Ludwig, F. Evers, A. Mildenerger, and A. D. Mirlin, Phys. Rev. Lett. **96**, 126802 (2006).
- ⁸ F. J. Wegner, Z. Phys. B **36**, 209 (1980); in *Localization and Metal Insulator Transitions*, edited by H. Fritzsche and D. Adler, Institute for Amorphous Studies Series (Plenum Press, New York, 1985).
- ⁹ C. Castellani and L. Peliti, J. Phys. A **19**, L429 (1986).
- ¹⁰ T. C. Halsey, M. H. Jensen, L. P. Kadanoff, I. Procaccia, and B. I. Shraiman, Phys. Rev. A **33**, 1141 (1986)
- ¹¹ A. Kudrolli, V. Kidambi, and S. Sridhar, Phys. Rev. Lett. **75**, 822 (1995).
- ¹² Y. V. Fyodorov and A. D. Mirlin, Phys. Rev. B **51**, 13403 (1995).
- ¹³ M. Schrieber and H. Grussbach, Phys. Rev. Lett. **67**, 607 (1991).
- ¹⁴ W. Pook and M. Janssen, Z. Phys. B **82**, 295 (1991).
- ¹⁵ F. Evers and A. D. Mirlin, Phys. Rev. Lett. **84**, 3690 (2000).
- ¹⁶ F. Evers, A. Mildenerger, and A. D. Mirlin, Phys. Rev. **64**, 241303(R) (2001).
- ¹⁷ A. Mildenerger, F. Evers, and A. D. Mirlin, Phys. Rev. B **66**, 033109 (2002).
- ¹⁸ H. Obuse, A. R. Subramaniam, A. Furusaki, I. A. Gruzberg, and A. W. W. Ludwig, Phys. Rev. Lett. **101**, 116802 (2008).
- ¹⁹ F. Evers, A. Mildenerger, and A. D. Mirlin, Phys. Rev. Lett. **101**, 116803 (2008).
- ²⁰ L. J. Vasquez, A. Rodriguez, and R. A. Römer, Phys. Rev. B **78**, 195106 (2008).
- ²¹ A. Rodriguez, L. J. Vasquez, and R. A. Römer, Phys. Rev. B **78**, 195107 (2008).
- ²² C. C. Chamon, C. Mudry, and X.-G. Wen, Phys. Rev. Lett. **77**, 4194 (1996).
- ²³ A. D. Mirlin and F. Evers, Phys. Rev. B **62**, 7920 (2000).
- ²⁴ I. I. Kogan, C. Mudry, and A. M. Tsvelik, Phys. Rev. Lett. **77**, 707 (1996).
- ²⁵ D. Carpentier and P. Le Doussal, Nucl. Phys. B **588**, 565 (2000).
- ²⁶ D. Carpentier and P. Le Doussal, Phys. Rev. E **63**, 026110 (2001).
- ²⁷ C. Mudry, S. Ryu, and A. Furusaki, Phys. Rev. B **67**, 064202 (2003).
- ²⁸ V. N. Prigodin and B. L. Altshuler, Phys. Rev. Lett. **80**, 1944 (1998).
- ²⁹ An analogous situation occurs for the random-energy model (REM),³⁰ where the *normalized* partition function $Z(\beta)/[Z(1)]^\beta$ plays the role of P_q [Eq. (1.1)] in the present work, with the identification $\beta \leftrightarrow q$; β denotes the inverse temperature in the REM. (A generalized REM describes delocalization in the 2D chiral Dirac model studied in Refs. 22,24,25,26,27,35,36,37,38,39,40; the connection is articulated in Refs. 22,26.) At high temperatures, $Z(\beta)$ is a self-averaging quantity with narrow statistics, though arbitrarily large moments of $Z(\beta)$ for *any* $\beta > 0$ suggest log-normal asymptotics.³⁰ For $\beta > \beta_c$, $Z(\beta)$ becomes broadly distributed.^{22,30} By contrast, the free energy $F = -T \ln Z$, in analogy with the typical $\tau(q)$ spectrum, remains narrowly distributed for all β .
- ³⁰ B. Derrida, Phys. Rev. Lett. **45**, 79 (1980); Phys. Rev. B **24**, 2613 (1981).
- ³¹ The averaged spectra $\bar{\tau}(q)$ defined in Eq.(1.3b) may exhibit a further “termination”, arising from the condition $\alpha \geq 0$; see e.g.: Ref. [3] and H. Obuse, A. R. Subramaniam, A. Furusaki, I. A. Gruzberg, and A. W. W. Ludwig, Physica E **40**, 1404 (2008).
- ³² A. M. M. Pruisken, Phys. Rev. B **31**, 426 (1985).
- ³³ D. Höf and F. Wegner, Nucl. Phys. B **275**, 561 (1986).
- ³⁴ F. Wegner, Nucl. Phys. B **280**, 193 (1987); **280**, 210 (1987).
- ³⁵ A. W. W. Ludwig, M. P. A. Fisher, R. Shankar, and G. Grinstein, Phys. Rev. B **50**, 7526 (1994).
- ³⁶ C. Mudry, C. Chamon and X.-G. Wen, Nucl. Phys. B **466**, 383 (1996).
- ³⁷ H. E. Castillo, C. C. Chamon, E. Fradkin, P. M. Goldbart, and C. Mudry, Phys. Rev. B **56**, 10668 (1997).
- ³⁸ O. Motrunich, K. Damle, and D. A. Huse, Phys. Rev. B **65**, 064206 (2002).
- ³⁹ T. Fukui, Phys. Rev. B **68**, 153307 (2003).
- ⁴⁰ H. Yamada and T. Fukui, Nucl. Phys. B **679**, 632 (2004).
- ⁴¹ Luca Dell’Anna, Nucl. Phys. B **750**, 213 (2006).
- ⁴² F. J. Wegner, Z. Phys. B **35**, 207 (1979).
- ⁴³ B. L. Altshuler, V. E. Kratsov, and I. V. Lerner, Pis’mma Zh. Eksp. Teor. Fiz. **43**, 342 (1986) [JETP Lett. **43**, 441 (1986)]; Zh. Eksp. Teor. Fiz. **91**, 2276 (1986) [Sov. Phys. JETP **64**, 1352 (1986)]; Phys. Lett. A **134**, 488 (1989).
- ⁴⁴ B. L. Altshuler, V. E. Kravtsov, and I. V. Lerner, in *Mesoscopic Phenomena in Solids*, edited by B. L. Altshuler, P. A. Lee, and R. A. Webb, North-Holland, Amsterdam, 449 (1991).
- ⁴⁵ F. Wegner, Z. Phys. B **44**, 9 (1981).
- ⁴⁶ A. J. McKane and M. Stone, Ann. Phys. (N.Y.) **131**, 36 (1981).
- ⁴⁷ In contrast, among the non-standard classes⁴⁸ extensively studied in the recent past, including the 2D Dirac models^{22,24,25,26,27,35,36,37,38,39,40} that inspired the present work, the average density of states may alternatively vanish or diverge at the delocalization transition, implying that $x_1^* \neq 0$. Eq. (1.5) applies equally to this more general case.
- ⁴⁸ M. R. Zirnbauer, J. Math. Phys. **37**, 4986 (1996); D. Bernard and A. LeClair, J. Phys. A **35**, 2555 (2002); A. Altland, B. D. Simons, and M. R. Zirnbauer, Phys. Rep. **359**, 283 (2002).
- ⁴⁹ Although the results for the symplectic symmetric class are also known, they have no direct physical application in Anderson localization. There is no perturbatively accessible, infra-red non-trivial fixed point in the symplectic symmetry class once the replica limit is taken.
- ⁵⁰ B. A. Muzykantskii and D. E. Khmel’nitskii, Phys. Rev. B **51**, 5480 (1994).
- ⁵¹ V. I. Fal’ko and K. B. Efetov, Europhys. Lett. **32**, 627 (1995); Phys. Rev. B **52**, 17413 (1996).
- ⁵² A. D. Mirlin, Phys. Rev. B **53**, 1186 (1995).
- ⁵³ B. Duplantier and A. W. W. Ludwig, Phys. Rev. Lett. **66**, 247 (1991).
- ⁵⁴ A. Kolmogorov, I. Petrovsky, and N. Piscounov, Moscow Univ. Math. Bull. (Engl. Transl.) **1**, 1 (1937).
- ⁵⁵ K. B. Efetov, A. I. Larkin, and D. E. Khmel’nitskii, Zh. Eksp. Teor. Fiz. **79**, 1120 (1980) [Sov. Phys. JETP **52**, 568 (1980)].
- ⁵⁶ A. M. Polyakov, Phys. Lett. **59B**, 79 (1975).
- ⁵⁷ See, e.g., E. Brézin, J. Zinn-Justin, and J. C. Le Guillou, Phys. Rev. D **14**, 2615 (1976); Phys. Rev. B **14**, 4976 (1976).
- ⁵⁸ See, e.g., J. Zinn-Justin, *Quantum Field Theory and Critical Phenomena*, 4th ed. (Oxford University Press, New York, 2002).
- ⁵⁹ The key to Eq. (2.16) is the standard angular momentum

addition formula

$$Y_{l_1, m_1}(\pi_+, \pi_-, \sigma) Y_{l_2, m_2}(\pi_+, \pi_-, \sigma) = \sum_{l, m} \langle l_1 l_2; l m | l_1 l_2; m_1 m_2 \rangle c_{l_1, l_2}^l Y_{l, m}(\pi_+, \pi_-, \sigma),$$

where $\langle l_1 l_2; l m | l_1 l_2; m_1 m_2 \rangle$ is a Clebsch-Gordan coefficient, and c_{l_1, l_2}^l is a normalization constant that is independent of $\{m, m_1, m_2\}$. As an example, one has

$$(\pi_+ + \pi_-)^2 = \frac{1}{\lambda_2} \left[Y_{2,2} - \sqrt{\frac{2}{3}} Y_{2,0} + Y_{2,-2} \right] + \frac{1}{\lambda_0} \frac{4}{3} Y_{0,0},$$

where the coefficients $\{\lambda_2, \lambda_0\}$ are determined by Eq. (2.18).

⁶⁰ Note, however, that for the O(3)/O(2) model, higher l operators possess *less* relevant scaling dimensions at the non-trivial critical point in $d = 2 + \epsilon$.⁵⁷ The existence of operators with arbitrarily negative scaling dimensions in the unitary class NL σ M emerges due to the replica $n \rightarrow 0$ limit.

⁶¹ Because of the symmetry restoration linking the ‘ π ’ (\hat{W}, \hat{W}^\dagger) and ‘ σ ’ ($\sqrt{\hat{\mathbb{I}}_n - \hat{W}\hat{W}^\dagger}, \sqrt{\hat{\mathbb{I}}_n - \hat{W}^\dagger\hat{W}}$) NL σ M fields at the non-trivial critical point in $d = 2 + \epsilon$ (for fixed $n \in \{1, 2, \dots\}$), many other eigenoperators exist that share the same “maximally” relevant eigenvalues as those defined by Eqs. (2.23) and (2.24). Our choice to focus upon the latter operator family is one of convenience.

⁶² J. Cardy, *Scaling and Renormalization in Statistical Physics* (Cambridge University Press, Cambridge, 1996); J. Cardy, “Conformal invariance and statistical mechanics,” in *Fields, strings and critical phenomena*, edited by E. Brézin and J. Zinn-Justin (Les-Houches 1988 XLIX); A. W. W. Ludwig and J. L. Cardy, Nucl. Phys. B **285**, 687 (1987).

⁶³ In principle, we could execute a straightforward (e.g. Wilsonian) renormalization group program upon the theory defined by Eqs. (2.7) and (2.27). In fact, a closely-related calculation was originally performed long ago, before the invention of the FRG, by Altshuler et al.^{43,44} within the context of mesoscopic fluctuations. These authors studied the time-reversal invariant (TRI) orthogonal class, and their calculation was complicated by the fact that they did not employ a basis of eigenoperators, such as those defined by Eq. (2.23) for the (different, broken TRI) unitary class; more importantly, they neglected the non-linear coupling between different moments implied by the OPE, Eq. (1.11).

It seems that a Wilsonian RG approach, such as that implemented in Ref. 44, does not produce as easily the features that we seek (such as, e.g. the lowest order fusion process $\mathcal{O}_1 \otimes \mathcal{O}_1 \rightarrow \mathcal{O}_2$, as represented by a term $\propto Y_1^2$ in the one-loop beta function for Y_2). Rather than using the FRG within the Wilsonian scheme, we deploy here the field theory approach explicated in Sec. V.

⁶⁴ A multi-local field theory, which can directly treat the probability distribution of the Green functions and the conductance, was proposed by Yudson in Ref. 65.

⁶⁵ V. I. Yudson, Phys. Rev. Lett., **94**, 156601 (2005).

⁶⁶ A. D. Mirlin and Y. V. Fyodorov, Phys. Rev. Lett. **72**, 526 (1994); V. Dobrosavljević and G. Kotliar, Phys. Rev. Lett. **78**, 3943 (1997).

⁶⁷ E. Brézin, S. Hikami, and J. Zinn-Justin, Nucl. Phys. B **165**, 528 (1980).

⁶⁸ Strictly speaking, the (bare, unrenormalized) matrix element in Eq. (5.8) is a mixed position and momentum space object, the precise definition of which is given by the correlation function

$$\Gamma_p^{(0)} \lambda_1 \dots \lambda_p [\mathcal{O}_p^{\alpha_1 \dots \alpha_p}(\mathbf{r})] = \frac{\langle \mathcal{O}_p^{\alpha_1 \dots \alpha_p}(\mathbf{r}) W^{\dagger \lambda_1 \gamma_1}(\mathbf{k}_1) \dots W^{\dagger \lambda_p \gamma_p}(\mathbf{k}_p) \rangle}{G(\mathbf{k}_1) G(\mathbf{k}_2) \dots G(\mathbf{k}_p)}, \quad (5.36)$$

where $G(\mathbf{k})$ is the “one-particle” propagator, which has the amplitude given by Eq. (5.1) at tree level. Only completely connected diagrams are counted in the evaluation of the right-hand side of Eq. (5.36). The external momenta $\{\mathbf{k}_1, \dots, \mathbf{k}_p\}$ can be taken to vanish in this equation.

⁶⁹ The tree level amplitude $\mathfrak{A}_p^{\lambda_1 \dots \lambda_p; \alpha_1 \dots \alpha_p}[\beta_1 \dots \beta_p]$ can be written as a sum of $2p$ -fold products of Kronecker delta functions. In the case of the operator $\mathcal{O}_2^{\alpha_1 \alpha_2}[\beta_1 \beta_2](\mathbf{r}) = (1/2!)^2 [W^{\alpha_1 \beta_1} W^{\alpha_2 \beta_2}(\mathbf{r}) - W^{\alpha_1 \beta_2} W^{\alpha_2 \beta_1}(\mathbf{r})]$, one finds the amplitude $\mathfrak{A}_2^{\lambda_1 \lambda_2; \alpha_1 \alpha_2}[\beta_1 \beta_2] = (1/2!)^2 [\delta_{\beta_1}^{\lambda_1} \delta_{\beta_2}^{\alpha_1} \delta_{\beta_1}^{\lambda_2} \delta_{\beta_2}^{\alpha_2} + \delta_{\beta_2}^{\lambda_1} \delta_{\beta_1}^{\alpha_2} \delta_{\beta_1}^{\lambda_2} \delta_{\beta_2}^{\alpha_1} - \delta_{\beta_2}^{\lambda_1} \delta_{\beta_1}^{\alpha_1} \delta_{\beta_1}^{\lambda_2} \delta_{\beta_2}^{\alpha_2} - \delta_{\beta_1}^{\lambda_1} \delta_{\beta_2}^{\alpha_2} \delta_{\beta_2}^{\lambda_2} \delta_{\beta_1}^{\alpha_1}]$.

⁷⁰ S. Elitzur, IAS preprint (1979).

⁷¹ A. McKane and M. Stone, Nucl. Phys. B **163**, 169 (1980).

⁷² D. J. Amit and G. B. Kotliar, Nucl. Phys. B **170**, 187 (1980).

⁷³ As discussed in Ref. 72, the basic problem is that non-invariant correlation functions suffer ultraviolet (UV) divergences for $d \geq 2$, and infrared (IR) divergences for $d \leq 2$ —there is no finite window of dimensionality free from both UV and IR problems. Within dimensional regularization, non-covariant correlators cannot be regularized via analytical continuation in d , so renormalized PT does not exist for these objects. By contrast, invariant correlators can be shown to be IR and UV finite for $0 < d < 2$; in this case, dimensional regularization works in the usual way.

⁷⁴ As an amusing aside, the same technique employed above can be used to derive the Gegenbauer polynomials, expanded in terms of $\vec{\pi}$ and $\sigma = 1 - \vec{\pi} \cdot \vec{\pi} / 2 + \dots$, in the O(n)/O($n-1$) model, given a knowledge only of the one-loop scaling dimension for composite eigenoperators belonging to a particular irreducible representation.

⁷⁵ Note that in order for the most relevant process in Eq. (5.23) to occur, it is necessary that all of the lower indices and all of the upper indices appearing on the LHS of this equation separately differ (i.e., no upper indices have the same value, no lower indices have the same value, but upper indices may take the same values as lower ones). Otherwise, the right-hand side of this equation vanishes, up to less relevant contributions.

⁷⁶ We neglect higher gradient operators throughout this paper, which are important to the computation of conductance, rather than LDOS fluctuations.^{43,44,77}

⁷⁷ F. Wegner, Nucl. Phys. B **354**, 441 (1991).

⁷⁸ Note that the OPE coefficient [Eq. (5.33)], and hence the coupled RG flow equations obtained in Sec. III [Eq. (3.5)], are similar to those obtained for the ‘chiral’ random vector potential and Class BDI 2D Dirac fermion models.²⁷ Indeed, the only qualitative difference is that the *average* of the LDOS acquires a relevant anomalous dimension in these chiral class models,^{27,35,38} whereas the unitary class is characterized by a non-critical average LDOS, which is

the consequence of the Ward identity. [See also the discussion following Eqs. (1.5)–(1.8b).]

⁷⁹ L. S. Brown, *Quantum Field Theory* (Cambridge University Press, New York, 1992).